RPP-RPT-30976, Revision 0

Surface Geophysical Exploration of S Tank Farm at the Hanford Site

D. Rucker
M. Levitt
hydroGEOPHYSICS, Inc.

C. Henderson
K. Williams
Columbia Energy & Environmental Services, Inc.

Date Published
September 2006

Post Office Box 1500
Richland, Washington

Prepared for the U.S. Department of Energy
Office of River Protection

Contract # DE-AC27-99RL14047, Modification M030

EXECUTIVE SUMMARY

During fiscal year 2006, a geophysical investigation was performed at the S tank farm on the U.S. Department of Energy's Hanford Site in Washington State. The objective of the investigation was to demonstrate the use of electrical resistivity methods to locate and map liquid injected into the tank farm vadose zone as a part of a simulated tank leak and to identify and map regions impacted by past leaks and spills. The geophysical methodology used on the S tank farm was the same as presented in *Surface Geophysical Exploration of T Tank Farm at the Hanford Site*.[1]

The leak injection test performed at the S tank farm is documented in *Tank 241-S-102 High-Resolution Resistivity Leak Detection and Monitoring Testing Report*.[2] The main purpose of the injection was to test the capabilities of the hydroGEOPHYSICS, Inc. high resolution resistivity - leak detection and monitoring (HRR-LDM) method for leak detection and leak quantification within a single-shell tank farm. The leak injection test consisted of a series of 10 injections, where a conductive fluid was discharged in well 40-02-10 near tank S-102. The LDM system was used to monitor the changes of electrical properties in the subsurface.

The electrical resistivity data acquisition phase for SGE included resistivity measurements on 8 surface electrode arrays oriented orthogonally and a set of 42 steel wells. The data collection concentrated primarily on the northern half of the S tank farm. Resistivity data were collected before, during, and after the leak injection test. Additionally, resistivity data collected using the HRR-LDM system after each of the 10 leak injections were analyzed using the SGE methodology to more fully understand the migration of the injected fluid.

Results of the test show that the resistivity data collected through surface arrays and via well-to-well (WTW) arrays can be used to locate and map the injection liquid. Additionally, the investigation identified other areas across the S tank farm that may be interpreted as contaminated regions.

The S tank farm SGE results are superior to those obtained for the T tank farm and documented in RPP-RPT-28955. While the analysis of surface data in the T tank farm investigation experienced significant interference problems with metallic infrastructure, this investigation had little interference. Thus, the three-dimensional representations can be evaluated using both surface data and WTW data. Analysis of both S and T farm results also demonstrated that WTW resistivity data has the capability to identify and delineate contaminant plume features within and around tank farms that have excessive metallic infrastructure such as pipes, tanks, diversion boxes, utilities, and cathodic protection.

Figure ES-1 shows the results of surface resistivity inversion modeling before (pre-leak) and after (post-leak) all leak injection testing. The figure shows a low resistivity plume beneath tank S-104, and how the low resistivity plume grows in size after the leak injection.

---

[1] RPP-RPT-28955, 2006, *Surface Geophysical Exploration of T Tank Farm at the Hanford Site*, Rev. 0, CH2M HILL Hanford Group, Inc., Richland, Washington.

[2] RPP-30121, 2006, *Tank 241-S-102 High-Resolution Resistivity Leak Detection and Monitoring Testing Report*, Rev. 0, CH2M HILL Hanford Group, Inc., Richland, Washington.

Figure ES-1. Views of Pre- and Post-LEAK Surface Inversion Results for the 1–2 ohm-m Level. A) Plan View; B) Side View; C) Three-Dimensional View.

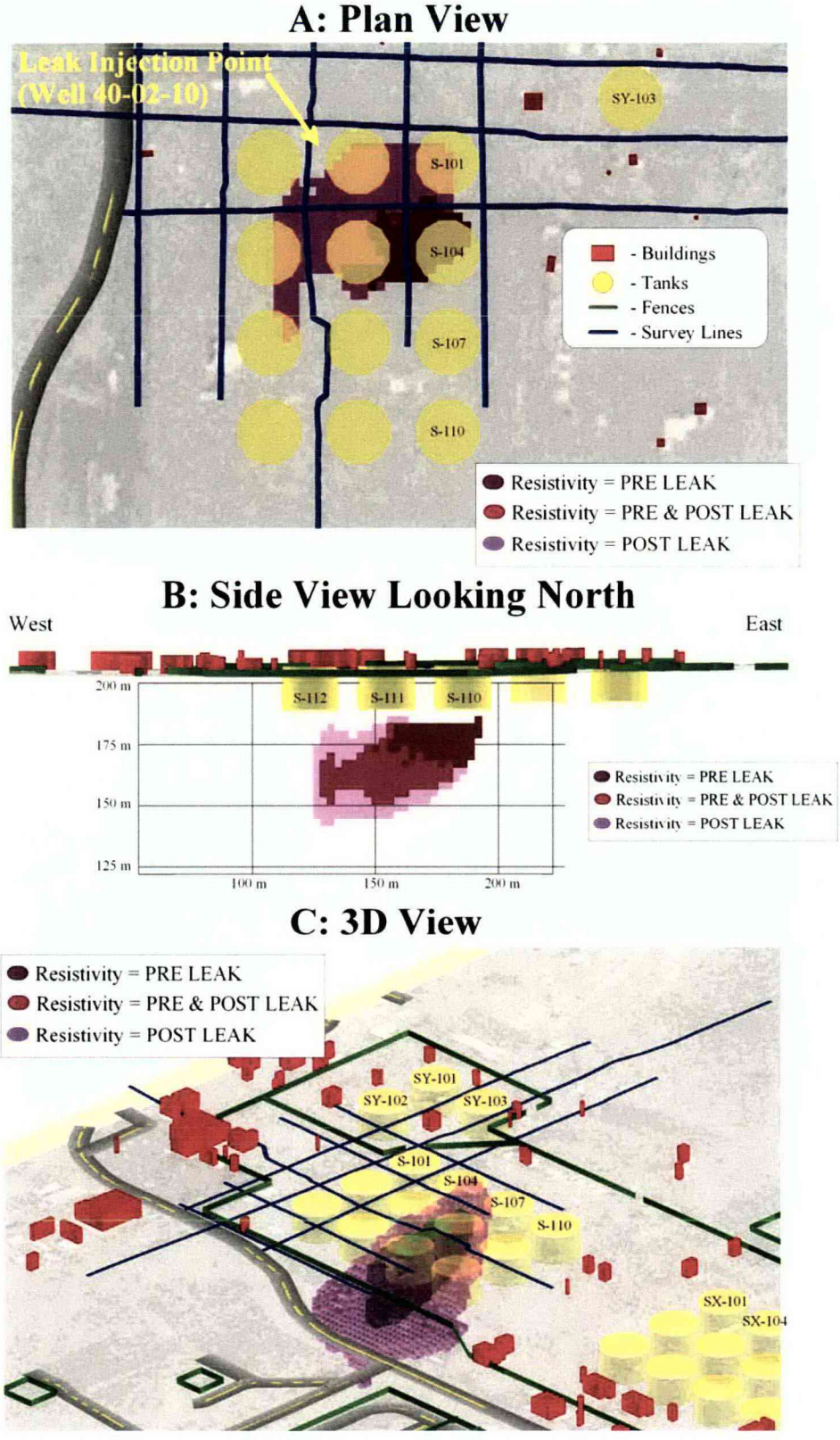

Figure ES-2 shows the results of the WTW inversion and the direct comparison with surface resistivity inversion results for both pre- and post-LEAK data sets. These results show that a majority of the low resistivity regions from the WTW and surface inversion overlap, giving a good indication of consistency among the two different electrode geometries. Those areas that do not overlap may be due to low resolution in data acquisition from either method or different coverage areas.

Figure ES-2. Direct Comparison of WTW Inversion with Surface Inversion, with WTW Opacity (red) of 1–14 ohm-meters and Surface Opacity (green) of 1–1.5 ohm-meters.

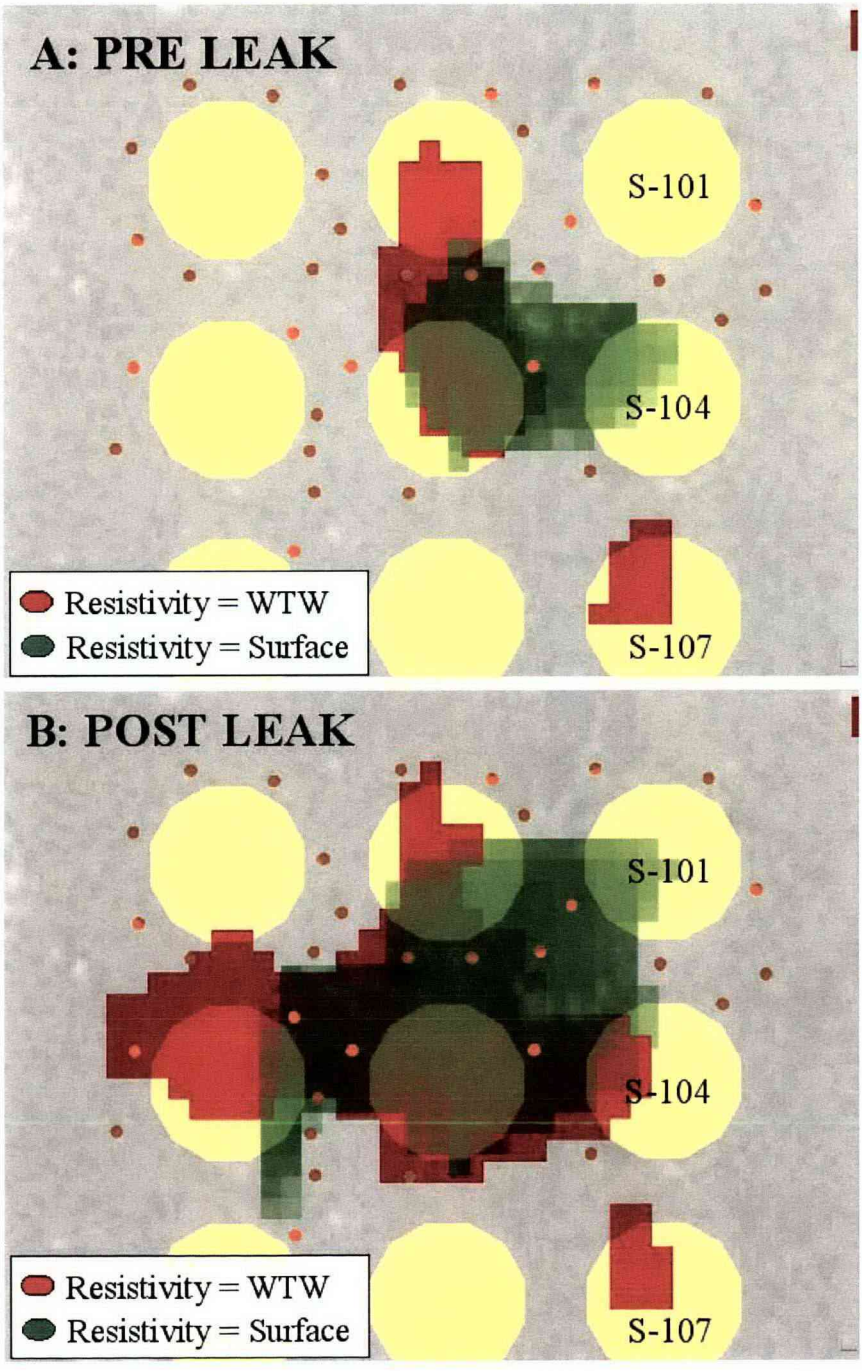

Several recommendations are suggested to improve the data acquisition, data quality, and data coverage of future SGE efforts at the Hanford Site tank farms.

- The success of SGE at both S and T tank farms lends credibility to the method for identifying historical leaks. It is recommended that all other farms be imaged with SGE, including a full-scale characterization of S tank farm.

- Install permanent surface electrodes within the farm to reduce time and costs for SGE deployment. This idea was first initiated for S tank farm and the strategy should continue to other farms.

- Computational power was limited for both S and T tank farms. It is recommended that the EarthImager3D code be fully parallelized to run on a multi-processor personal computer with extended random access memory.

- Resistivity data collected with the HRR-LDM system were evaluated with a processing methodology developed primarily for SGE data. It is recommended that a larger LDM hardware system be developed that can monitor/characterize an entire farm, where SGE-type processing can be performed at pre-determined intervals to ensure that no leaks are occurring during retrieval.

- Vertical resolution is relatively low (compared to lateral resolution) for the surface resistivity data collection and non-existent for WTW resistivity. It is recommended that as many subsurface point electrodes be installed as possible, including electrical resistivity tomography (ERT) arrays that have many point electrodes along a single borehole. The ERT arrays would increase vertical resolution.

TABLE OF CONTENTS

LIST OF APPENDICES

LIST OF FIGURES

LIST OF TABLES

LIST OF TERMS

Terms

Conductivity. The ability of a material to transmit or conduct an electric impulse; reciprocal of resistivity.

Inversion. Inversion, or inverse modeling, attempts to reconstruct subsurface features from a given set of geophysical measurements, and to do so in a manner that the model response fits the observations according to some measure of error.

Petrophysical. Petrophysics pertains to the determination of physical properties of rocks through various geophysical methods including laboratory studies, borehole investigations, and/or field surveys.

Resistance. The opposition of a material to current passing through it; received voltage normalized by transmitted current.

Resistivity. A material property that is measured as its resistance to current per unit length for a uniform cross section; reciprocal of conductivity.

SuperSting R8 IP. SuperSting R8 resistivity and induced polarization meter produced by Advanced Geosciences, Inc.

Tomography. A method of producing a three-dimensional image of a volumetric object (plume) by the observation and recording of the differences in the effects on the passage of waves of energy impinging on that object.

Abbreviations, Acronyms, and Initialisms

AWG	American wire gauge
CH2M HILL	CH2M HILL Hanford Group, Inc.
DOE	U.S. Department of Energy
ERT	electrical resistivity tomography
HGI	hydroGEOPHYSICS, Inc. of Tucson, Arizona
HRR	high-resolution resistivity
LDM	leak detection and monitoring
PUREX	plutonium-uranium extraction
REDOX	reduction-oxidation
SGE	surface geophysical exploration
SST	single-shell tank
V/I	voltage potential
WTS	well-to-surface
WTW	well-to-well

1.0 INTRODUCTION

Beginning in December 2005 and ending in August 2006, a geophysical study was completed at the 241-S tank farm at the U.S. Department of Energy (DOE) Hanford Site in eastern Washington State. Columbia Energy & Environmental Services, Inc. of Richland, Washington, and hydroGEOPHYSICS, Inc. (HGI) of Tucson, Arizona, with support from CH2M HILL Hanford Group, Inc. (CH2M HILL) conducted geophysical surveys of the S tank farm, located in the 200 West Area of the Hanford Site. The geophysical surveys consisted of electrical resistivity surveying on a set of 8 orthogonal surface lines and 42 wells. The geophysical survey focused primarily on the northern portion of the site near tanks S-101 through S-106. The geophysical survey was conducted before, during, and after a planned leak injection test near tank S-102 in an effort to locate and map the migration of the injected fluid. A description of the leak injection test is provided in RPP-30121, *Tank 241-S-102 High-Resolution Resistivity Leak Detection and Monitoring Testing*, and CEES-0320, *Test Report for the Leak Injection Test at Tank 241-S-102*.

1.1 SCOPE

The scope of the geophysical surveying was completed within three main tasks. The surveying encompassed data acquisition on both surface electrodes and wells, data processing (i.e., quality assurance, quality control, data reduction, and electrical resistivity inversion modeling), and visualization (i.e., either two-dimensional contour plots of individual resistivity lines, two-dimensional contour plots of well-to-well [WTW] inversion plots, or rendered three-dimensional solid model plumes). The first task (Task I) included a pre-injection survey to establish baseline conditions around the S tank farm, concentrating mainly on the north side of the farm where the fluid injection was planned. The baseline conditions would be used to compare with future surveys and is referred to as the "pre-leak" survey. The second task (Task II) included an experiment to test the sensitivity of the surface resistivity method to very small changes in the subsurface electrical properties. This task included measurements on only two orthogonal surface lines near an injection well. The well was used as a reverse well to pump an electrically conductive sodium thiosulfate solution below the base of tank S-102 in well 40-02-10. This task is referred to as the "mid-leak" survey.

The third task (Task III), referred to as the "post-leak" survey, repeated the baseline surveying effort in scope after the completion of the leak injection testing. The leak injection included approximately 13,000 gallons in a series of 10 injections between January and April 2006. The results of the post-leak survey were compared to the pre-leak survey by qualitatively comparing the size of a specific resistivity contour value or quantitatively by differencing the results directly.

1.2 OBJECTIVES

The two main objectives for this geophysical investigation included:

- Utilize surface geophysical exploration (SGE) methods to locate and map the fluid injected near tank S-102 and correlate the results to the known volume of liquid injected into the subsurface.
- Utilize SGE methods to identify and map contamination in the subsurface in and around the S tank farm prior to a leak injection to establish baseline conditions

1.3 REPORT LAYOUT

This report is divided into seven main sections.

- **Section 1.0, Introduction** – Describes the scope and objectives of the investigation.
- **Section 2.0, Background** – Describes the setting of the S tank farm, with geology and hydrology, and information regarding the disposal activities in and around the tank farm.
- **Section 3.0, Data Collection** – Discusses the methodology and logistics of conducting the geophysical survey at the S tank farm.
- **Section 4.0, Analysis Results and Interpretation** – Presents the results from the surveying effort.
- **Section 5.0, Conclusions** – Provides conclusions drawn from the results, interpretations, and subsequent assessment of results.
- **Section 6.0, Recommendations** – Provides recommendations for improving follow-on SGE efforts.
- **Section 7.0, References** – Lists reference documents cited in the report.

2.0 BACKGROUND

The 241-S tank farm is 1 of 12 single-shell tank (SST) farms on the Hanford Site. The tank farm was constructed to store highly radioactive waste generated by chemical processing of irradiated uranium fuel. The S tank farm is located in the southwest portion of the 200 West Area, northwest of S Plant (Figure 1). Construction of the S tank farm was completed during 1950–1951. The site is surrounded by a number of cribs and specific-retention trenches and cribs. Most of the cribs and all of the specific-retention trenches received wastes directly from SSTs (WHC-MR-0227, *Tank Wastes Discharged Directly to the Soil at the Hanford Site*).

Figure 1. S Tank Farm Complex Base Map including S, SX, and SY Tank Farms.

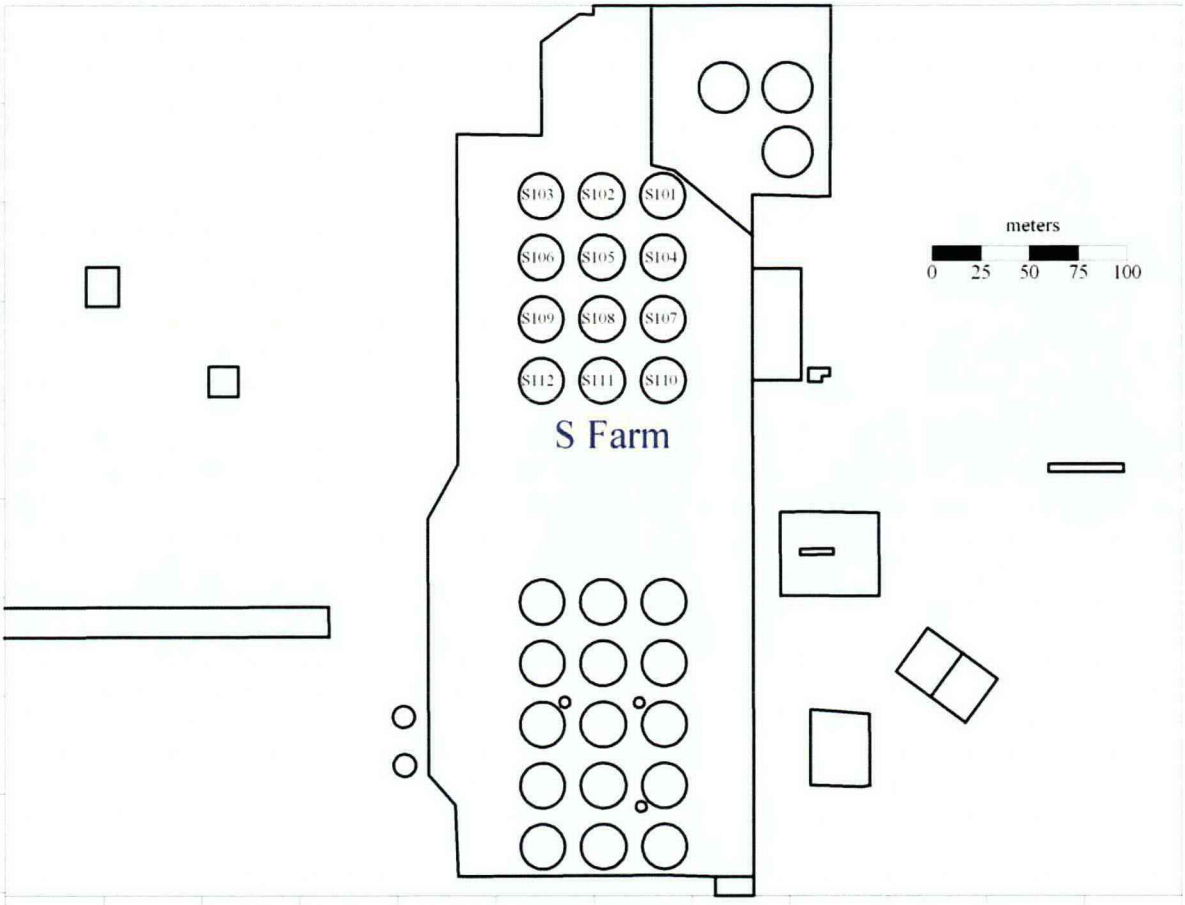

The CH2M HILL Tank Farm Vadose Zone Project has the responsibility for all projects associated with vadose zone characterization at the tank farms under the direction of the DOE Office of River Protection. Pacific Northwest National Laboratory is currently responsible for all groundwater monitoring at the tank farms and is integrated with the Tank Farm Vadose Zone Project through the Hanford Groundwater Remediation Project, under the direction of the DOE Richland Operations Office.

The S tank farm comprises the following:

- 12 SSTs each with a 2.86 x 10^6-liter (758,000-gallon) capacity (Figure 2)
- Waste transfer lines
- Leak detection systems
- Tank ancillary equipment.

The basic tank structure consists of a carbon steel liner covered with a reinforced concrete shell that completely encases the steel liner and extends continuously above the liner wall to form a dome cover over the tank. Between the steel liner and concrete shell is a 3/8-inch-thick asphalt membrane that serves as a waterproofing layer. The tanks are situated entirely below surface, with a base at approximately 13.7 meters (45 feet) below ground surface. The top of the

concrete tank dome covered with about 2.4 meters (8 feet) of backfill. Historical data on the S tank farm including the infrastructure, waste management practices, and geologic setting are provided in HNF-4936, *Subsurface Physical Conditions Description of the S-SX Waste Management Area* and RPP-7884, *Field Investigation Report for Waste Management Area S-SX.*

The backfill that covers the SSTs came from screened (i.e., large stones removed), excavated soil material. The heavy equipment that was used for excavation and for completing the tank construction is thought to have produced a compaction layer under and around each tank. The backfill between and over the tanks is relatively homogeneous compared with the undisturbed soil under the tanks.

Figure 2. S Tank Farm 758,000-gallon Tank.

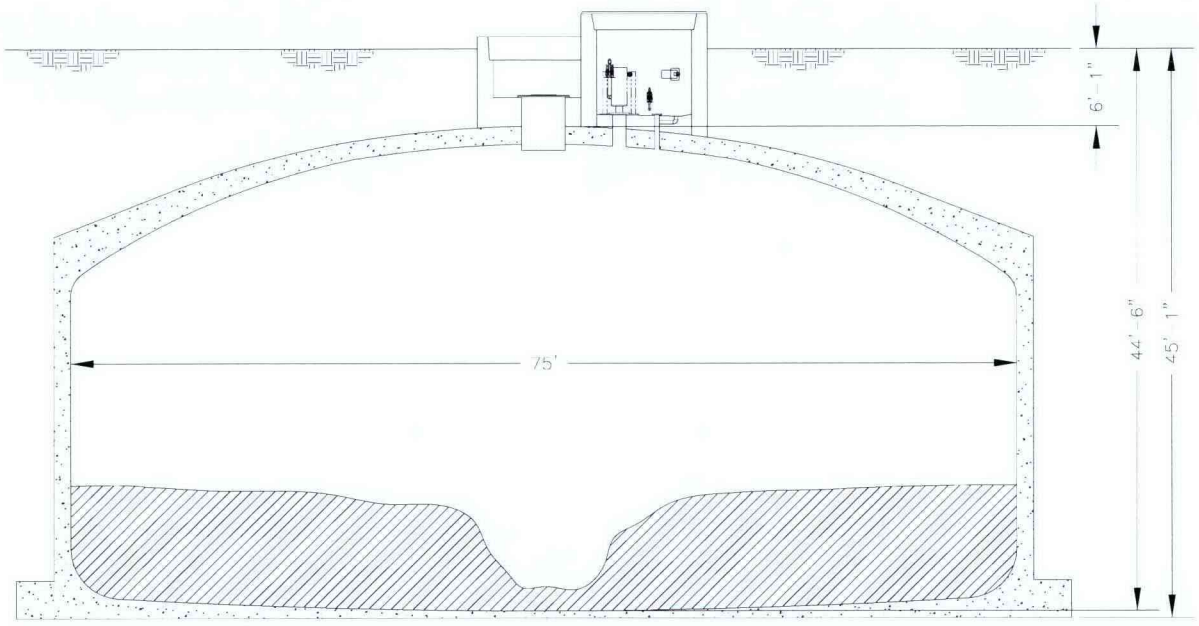

The S farm tanks are connected in four three-tank cascade series that are arranged with each successive tank sited at a lower elevation. Each tank is surrounded by several boreholes in which radiometric instruments were used to detect changes in activity levels in the sediments surrounding the borehole. Seventy-one boreholes were constructed between 1952 and 1978 to monitor for leaks from the 12 SSTs of the S tank farm. These boreholes served as both primary and secondary leak detection devices. For example, HGI used the wells around tank S-102 for an electrically-based leak detection system (CEES-0320).

2.1 TANK CONTENTS

Radioactive waste generated at the Hanford Site from 1945 to 1989 was derived predominantly from the chemical dissolution and extraction of plutonium and uranium from irradiated reactor fuel elements. The extractions during these years evolved through three basic processes: the bismuth phosphate (BiPO4) process, the reduction-oxidation (REDOX) process, and the

plutonium uranium extraction (PUREX) process. The S tank farm received waste primarily from the REDOX process from the REDOX plant. The REDOX plant was the first plant to separate both plutonium and uranium using solvent extraction.

The waste in the S tank farm consists mainly of sludge, salt cake, and liquid. Sludge is composed of solid precipitate (hydrous metal oxides) that results from the neutralization of acid waste. The wastes were neutralized before being transferred to the waste tanks. Salt cake is composed of salts formed by the evaporation of water from the waste. Sludge and salt cake form the solids component of the tank waste. Liquids are present as supernate and interstitial liquids. The supernate, which is found on the top of the solid waste surface, has been pumped to double-shell tanks. Interstitial liquid fills the interstitial spaces within the waste solids. Interstitial liquid may be drainable if it is not held in the void spaces by capillary forces.

General tank content (i.e., liquid and solid volumes) data and some tank monitoring data are summarized monthly in waste tank summary reports (e.g., HNF-EP-0182, *Waste Tank Summary Report for Month Ending June 30, 2006*). Tank S-104 is the only S tank farm tank that is classified as a leaker. This tank is currently estimated to have leaked a total of 90,850 liters (24,000 gallons) of tank waste.

The tanks in the S tank farm currently contain an estimated total volume of 15×10^6 liters (3,969,000 gallons) of mixed wastes consisting of various REDOX waste streams, various wastes from other SST farms, and 242-S Evaporator/Crystallizer waste streams.

2.2 FLUID DISCHARGE TO S AND SX TANK FARMS

The following description of fluid disposal to the S and SX tank farms (including adjacent waste areas) is from HNF-4936:

> "...there are a number of cribs around the S-SX WMA that received large volumes of slightly contaminated water and other waste streams. Historical records indicate that tank wastes were not cascaded from the boiling tanks into cribs. Rather the cribs received excess condensate from the boiling waste tanks and cooling water from the condensers. Liquids were transferred through a complex piping system that includes collection boxes (e.g., diversion boxes, valves, pits) for routing liquids to various locations. Other additions to the cribs included discharges from the first cold REDOX start-up run and groundwater coming from the U-crib "pump and treat" operations in the mid-1980s...
>
> In addition, the U-10 pond received about 44 billion gallons of slightly contaminated water, a fraction of which included fluids generated by S-SX Tank Farm operations. The large additions of water to the U-10 pond significantly impacted groundwater flow patterns under the S-SX WMA.
>
> Finally, a number of raw and potable water lines are present in the S-SX WMA vicinity. Leaks from lines could have contributed to tank waste migration in the vadose zone. It appears that leaks from the lines were not viewed as having adverse impacts to tank farm operations. Thus, historical records are likely to be incomplete."

Figure 3 was generated from data presented in Table 2-1 of HNF-4936. One change was made, however, which updated the disposal of tank S-104 from 22,700 to 90,800 liters (6,000 to 24,000 gallons) (HNF-EP-0182). Another notable feature of the figure is the unknown volumetric spill near tank S-102 from near-surface pipelines or tank flanges. This leak and the resulting cleanup actions is documented in ARH-2977, *Report on the Cleanup Activities Following the 241-S Tank Farm Contamination Occurrence at the Hanford Reservation Richland, Washington on November 14, 1973*. The leak was estimated at 8,600 gallons of high salt waste that overflowed a riser onto the surface. Cleanup actions were performed to excavate and package the contaminated soil. However, it is not known how much of the soluble salts were transported into the vadose zone from the application of water used for dust and contamination control. Lastly, a water line rupture occurred in 1996 that released an estimated 1.9×10^6 liters (500,000 gallons) of raw water over a 1-hour period (HNF-4936). Water flowed into the north end of the S tank farm. Most of the water infiltrated along the east side of the S tank farm.

Figure 3. Surficial Fluid Discharge Summary (m^3) to S and SX Tank Farms. (Size of dot is proportional to the volume released.)

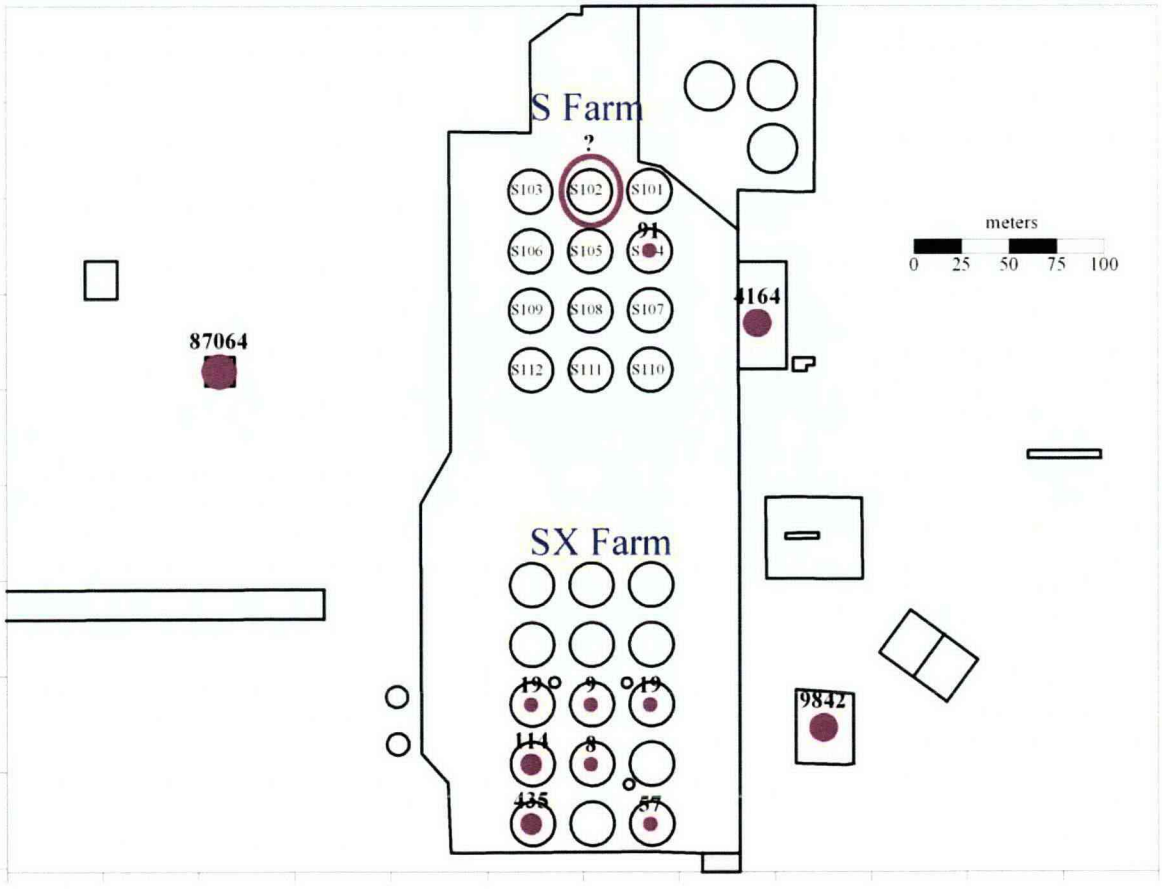

As a result of the discharges around S and SX tank farms, some of the inorganic tank and crib constituents reached the groundwater. Figure 4 shows the distribution of nitrate from recent (2004) groundwater data (PNNL-15670, *Hanford Site Groundwater Monitoring for Fiscal Year 2005*). The figure was created by interpolating the data over the entire 200 West Area using a linear variogram fit with a nugget effect. Two main conclusions can be drawn from the figure, the large nitrate concentration plume west of SX tank farm, and the lack of any data within S tank farm. The interpolation through the S tank farm is highly suspect and it unknown whether any discharge from the farm (i.e., tank S-104) reached the water table.

Figure 4. Groundwater Nitrate Concentrations around S and SX Tank Farms.

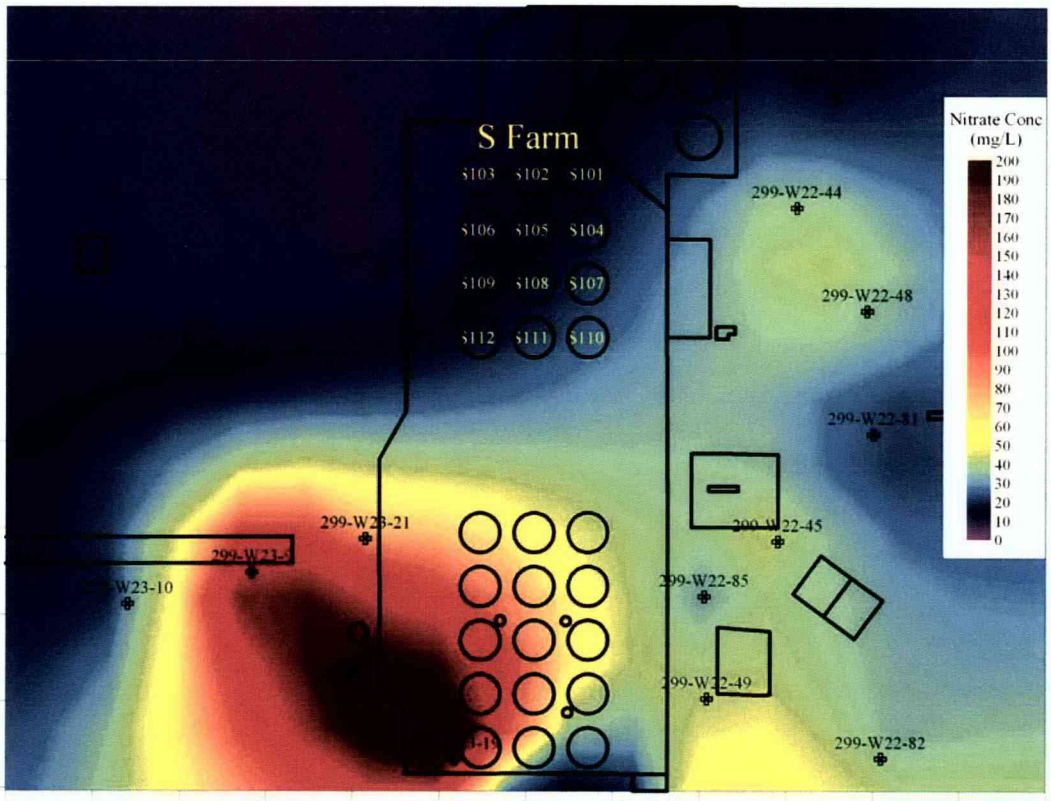

2.3 LEAK INJECTION TEST

The leak detection and monitoring (LDM) leak injection test commenced on January 20, 2006, with an initial injection of 3,050 gallons of sodium thiosulfate released via a modified drywell. The injection depth was approximately 15.24 meters (50 feet), immediately below the toe of the S-102 tank. The simulated waste consisted of solution of 25% (by volume) sodium thiosulfate pentahydrate with a specific gravity of approximately 1.138 at a temperature of 23.1 degrees Celsius. The waste simulant had conductive properties substantively similar to the radioactive waste stored in underground tanks. A comprehensive description of the leak injection test schedule, equipment, and methodology can be viewed in RPP-30121. Table 1 contains a summary of the leak injection test schedule and injection volumes.

Table 1. Summary of HRR-LDM Leak Injection Schedule and Volumes.

Activity	Start Date/Time	Stop Date/Time	Approximate Leak Rate (gallons per hour)	Operating Duration (hours)	Approximate Volume (gallons)	Approximate Cumulative Volume (gallons)
Leak Test 1	1/20/06 at 1820	2/2/06 at 0620	10	300	3050	3050
Leak Test 2	2/13/06 at 1015	2/18/06 at 0915	15	119	1750	4800
Leak Test 3	3/7/06 at 1210	3/15/06 at 1320	5	193.17	1000	5800
Leak Test 4	3/21/06 at 0815	3/23/06 at 0950	20	49.58	1000	6800
Leak Test 5	4/12/06 at 1000	4/14/06 at 1200	20	50	1000	7800
Leak Test 6	4/19/06 at 0825	4/23/06 at 1140	10	99.25	1025	8825
Leak Test 7 [a]	4/27/06 at 1230	5/2/06 at 1400	10	117	1200	10,025
Leak Test 8	5/8/06 at 1300	5/11/06 at 0920	15	68.33	1050	11,075
Leak Test 9 [b]	5/15/06 at 1700	5/19/06 at 0800	5/15	18/63	1050	12,125
Leak Test 10	5/23/06 at 1000	5/25/06 at 1030	20	48.5	1025	13,150

Notes:

[a] A series of four stop/restarts were performed following the initiation of leak test 7. The associated times for the leak rate stops and restarts were as follows: stop 4/27 at 1630, restart at 1800; stop 4/28 at 0800, restart at 0930; stop at 1100, restart at 1230; stop at 1400, restart at 1500.

[b] A series of two stop/restarts were performed following the initiation of leak test 9 at 5 gallons per hour. The associated times for the leak rate stops and restarts were as follows: stop 5/16 at 0800, restart at 1000; stop at 1200 and restart at 1400. The flow rate for leak test 9 was increased from 5 to 15 gallons per hour on 5/16 at 1500. One stop/restart cycle was performed at the higher flow rate. The associated times for the leak rate stop and restart were as follows: stop 5/18 at 1130 and restart at 1330.

HRR-LDM = high resolution resistivity - leak detection and monitoring.

3.0 DATA COLLECTION

3.1 SURVEY AREA AND COVERAGE

The survey area was limited to the northern half of S tank farm that immediately surrounds the S-102 leak injection area. The geophysical survey included 8 high resolution resistivity (HRR) surface electrode lines and 42 wells, including 34 drywells and 8 groundwater wells. A summary of the data collection phases, methods, and survey coverage area can be viewed in Table 2. The survey line layout and well locations are presented in Figure 5. Table 3 lists the specific wells used in this effort.

Table 2. Summary of Data Coverage.

Survey Phase	Date	Surface HRR			Well Tomography		
		No. Survey Lines & Total Coverage	Average Line & Electrode Spacing	No. Data Points	No. Wells	Well Spacing	No. Data Points
Pre-leak	12/14/05 to 1/3/06	8 1.8 km	34 m 3 m	22,000	41	5 – 300 m	1,600
Mid-leak	2/23/06 to 2/24/06	2 0.4 km	NA 3m	3,800	None	None	None
Post-leak	6/12/06 to 6/20/06	8 1.8 km	34 m 3 m	25,000	42	5 – 300 m	1,600

Notes:
HRR = high-resolution resistivity.
km = kilometer.
m = meter.
NA = not applicable.

Table 2. Wells Used for Pre- and Post-SGE Survey.

Well Number	Post-Leak Well	Well Number	Post-Leak Well
1	40-00-02	22	40-04-08
2	40-01-01	23	40-05-03
3	40-01-04	24	40-05-07
4	40-01-06	25	40-05-08
5	40-01-08	26	40-05-10
6	40-01-10	27	40-06-02
7	40-02-01	28	40-06-04
8	40-02-03	29	40-06-05
9	40-02-04	30	40-06-08
10	40-02-05	31	40-06-09
11	40-02-07	32	40-08-09
12	40-02-08	33	40-09-02
13	40-02-11	34	W-22-44
14	40-03-01	35	W-22-48
15	40-03-03	36	W-22-81
16	40-03-05	37	W-22-84
17	40-03-06	38	W-23-1
18	40-03-08	39	W-23-7
19	40-03-09	40	W-23-20
20	40-03-11	41	W-23-21
21	40-04-01	42	40-02-10

Note: Well 40 (W-23-20) was not used during the pre-leak injection data collection and was used during the post-leak injection data collection.

Figure 5. Geophysical Data Collection Area Showing Location of HRR Survey Lines and Wells.

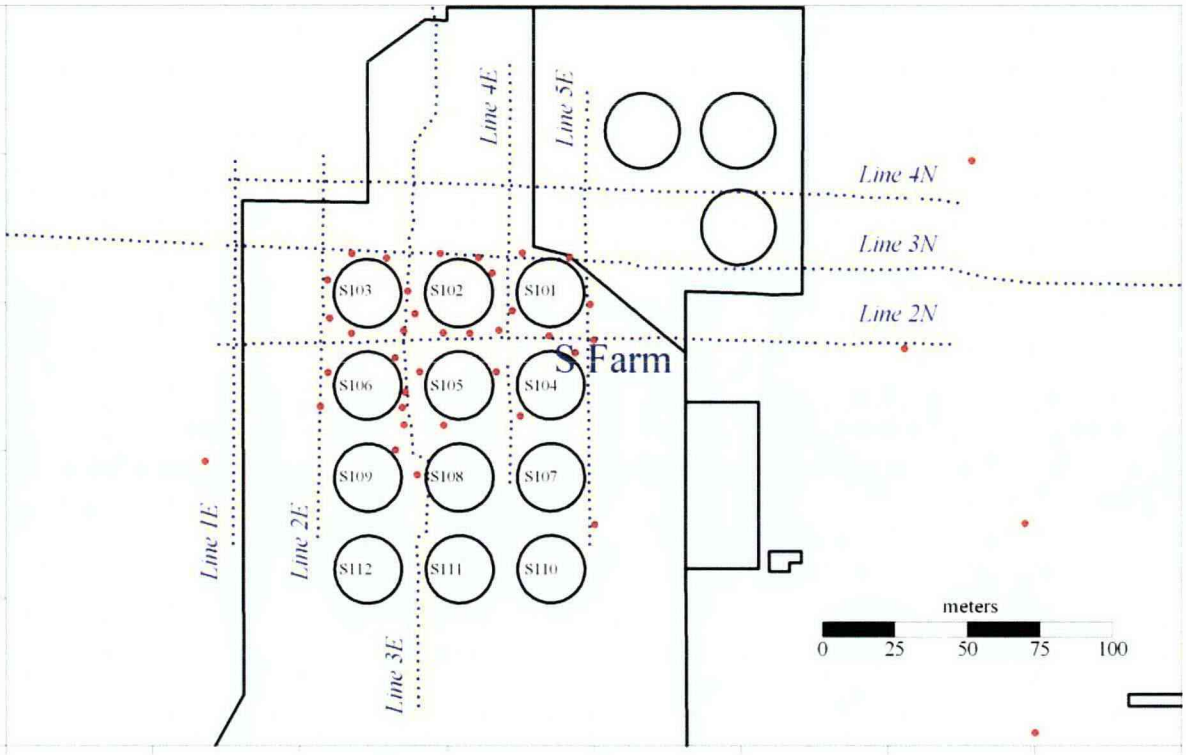

Table 4 contains a summary of data acquisition parameters including line direction, number of electrodes, and line lengths.

Table 4. Summary of Data Acquisition Parameters.

Line	Direction	Well-to-Surface	Pre-Leak & Post-Leak		Mid-Leak	
			Number of Electrodes	Length (meters)	Number of Electrodes	Length (meters)
Line 1N	North-South	NA	NA	NA	None	None
Line 2N	North-South	Yes	84	249	None	None
Line 3N	North-South	Yes	140	417	None	None
Line 4N	North-South	Yes	249	84	None	None
Line 1E	East-West	No	44	129	None	None
Line 2E	East-West	No	44	129	None	None
Line 3E	East-West	No	102	303	102	303
Line 4E	East-West	No	48	141	48	141
Line 5E	East-West	No	52	153	None	None

NA = not applicable.

3.2 INSTALLATION AND SETUP

3.2.1 Temporary Installation of Remote Reference Arrays

The project began on December 11, 2005, by establishing the remote reference electrode arrays to the southwest and the southeast of the S tank farm site. Two grounded remote reference electrode arrays were installed approximately 1.1 miles (1.7 kilometers) from the survey area and connected via 16 American wire gauge (AWG) machine tool wire. A more detailed description of the installation practice can be viewed in RPP-RPT-28955, *Surface Geophysical Exploration of T Tank Farm at the Hanford Site*.

3.2.2 Survey Design and Layout

The geophysical survey design, which included the location and spatial coverage of the geophysical electrodes, was a compromise between a number of factors including:

- The desire to provide sufficient survey coverage to adequately image the historic leak events (tank S-104)
- The desire to provide sufficient survey coverage to adequately image the injection leak fluid volume in the area between tanks S-102 and S-103
- The desire to limit the data acquisition time and disruption to tank farm activities and balance SGE data collection with HRR-LDM monitoring (HRR-LDM cannot operate simultaneously with SGE).

3.2.3 Temporary versus Permanent Surface Electrodes

Temporary surface electrodes (i.e., electrodes that were removed after data acquisition was complete) were initially installed along the eight surface HRR lines as part of the pre-leak and mid-leak injection test phases. Permanent surface electrodes were installed along all eight survey lines as part of the post-leak injection phase. Temporary and permanent electrodes were fabricated out of stainless steel rod and were installed to the same depth.

3.3 RESISTIVITY EQUIPMENT

Electrical measurements were acquired using a SuperSting R8[3] in pole-pole array configuration. A combination of passive cables using automated electrode switching boxes, and active cables where the electrode switching is performed on the cable, were used to connect the surface electrodes to the SuperSting R8 data acquisition unit. Two 12-volt direct current marine deep

[3] SuperSting R8 and SuperSting R8 IP are trademarks of Advanced Geosciences, Inc., Austin, Texas.

cycle batteries were used to supply input power. The batteries and power cable were strictly controlled using appropriate lockout and tagout procedures. A more comprehensive description of the equipment can be viewed in RPP-RPT-28955.

3.4 PRE-LEAK GEOPHYSICAL SURVEYING

Onsite activities commenced on December 11, 2005, with the preparation of wells that were used in collecting WTW and well-to-surface (WTS) data. A total of 41 wells were used for data collection, including 34 drywells, and 7 groundwater wells. A list of the specific wells used for data collection is provided in Table 3. In addition to the wells, eight surface electrode survey lines were deployed. Data acquisition for the pre-leak phase was performed between December 14, 2005, and January 3, 2006.

Specifically for the WTW geophysical survey, individual 16 or 18 AWG machine tool wire was run from a central location outside the S tank farm fence to each of the 41 wells. Each well was prepared by removing a small area of rust from the inside of the well casing, and a short length of bare wire was wedged between the inside diameter of the casing and the well plug. Standard electrical wire nuts were used to connect the wire to the bare wire. The wires were then routed outside the tank farm and connected to a distribution panel, which in turn was connected to a SuperSting switch box. The switch box acts as a multiplexor that distributes the measurements logically according to the SuperSting R8. Figure 6 is a photo showing the equipment setup and wire-to-well connection. Both WTW and WTS measurement sets were acquired under one configuration. For logistical reasons, WTS data was only acquired for lines 2N, 3N, and 4N.

Figure 6. Equipment and Setup for the Well-to-Well Survey.

The pre-leak survey weather conditions included snow, ice, and freezing rain with temperatures ranging from 12 to 40 degrees Fahrenheit. Weather related equipment failure occurred while acquiring survey line 1N and produced substandard data that could not be salvaged. Figure 7 is a photo showing the environmental conditions under which the survey was completed.

Figure 7. Environmental Conditions during the Pre-Leak Survey.

3.5 MID-LEAK GEOPHYSICAL SURVEYING

The mid-leak SGE data acquisition phase was completed between February 23, 2006, and February 24, 2006, between injection leaks 2 and 3, after 4,800 gallons had been released. A portion of survey lines 3E and 3N were re-acquired to assess whether any detectable change due to a small amount of injected volume could be detected. No well data was acquired for the mid-leak, other than the LDM data collected around tank S-102.

3.6 POST-LEAK GEOPHYSICAL SURVEYING

The last HRR-LDM leak injection test was completed on May 25, 2006, with a cumulative volume of 13,150 gallons. Data from the 8 surface lines and 42 wells that were a used for the pre-leak survey were re-acquired using the same wells and surface electrode locations so that a direct comparison could be performed. The post-leak SGE data acquisition commenced on June 12, 2006, approximately 18 days after completion of the leak injection test.

Permanent surface electrodes were installed along all eight survey lines to streamline the data acquisition activities and improve future data acquisition repeatability. Each electrode consisted of 1/2-inch diameter stainless steel rod in the shape of a "T." The top horizontal bar rested on the ground surface, increasing electrode to ground contact and limiting the electrode penetration to 11 inches. The top bar also provided a suitable location for connecting the data acquisition cable.

4.0 ANALYSIS RESULTS AND INTERPRETATION

This section presents the analysis results along with interpretation of the results.
The methodology used for the S tank farm investigation parallels the recently completed SGE investigation of the T tank farm. A description of the data processing methods, theory, and limitations associated with using electrical resistivity methods in a tank farm environment are described in RPP-RPT-28955.

4.1 SURFACE ELECTRICAL RESISTIVITY INVERSION

Prior to the leak injection at the S-102 tank, a set of eight orthogonal HRR lines were acquired using the pole-pole array. The data were collected in a two-dimensional arrangement, which is logistically easier and more cost effective due to the reduced equipment requirements relative to a fully three-dimensional data acquisition effort. The pre-leak HRR collection efforts included lines 2N-4N and 1E-5E. Initially, resistivity data collection was to be completed on lines 1N and 5N, but extreme adverse weather conditions prevented data collection at these two lines.

Figures A-1 through A-8 in Appendix A show the HRR pre-leak data, plotted as apparent resistivity according to the common HRR plotting methodology presented in RPP-RPT-28955.

The next step for evaluation was to filter the data set to remove spikes and data with high repeatability error. Filtering was accomplished by plotting all receivers associated with a particular transmitter. Using Figure 8A as a guide, a single transmitter is shown with a series of receivers. The distance between a transmitter-receiver pair will dictate the depth at which the data point is represented. Figure 8B shows how the entire subsurface is filled in when considering all transmitter-receiver pairs. Figure 8C shows a plot of the actual normalized voltage potential (V/I in ohms [transfer resistance]) associated with a transmitter. Within the plot is an example set from both S and T tank farms. For the S tank farm data set, a single spike is seen for the receiver located at approximately 75 meters along the HRR line. The spike violates potential field theory, and therefore is likely due to measurement error. Potential field theory, in summary, states that if the spike would have been from a very resistive layer, then it would also have influence on all other measurements at larger separations, which is not the case in Figure 8C. For filtering, this spike is rejected from the data set due to its noisy nature. Normally, these spikes will carry through a series of transmitters and may be associated with one receiver. For this case, the data for the entire receiver was deleted.

Figure 8C also shows the results of a T tank farm transmitter within line 4E. This line was located between the 100- and 200-series tanks and was oriented in the north-to-south direction. The V/I at large distances, which coincides with lower V/I values, are extremely noisy. Little confidence can be placed in data values less than 0.1 ohms for this particular transmitter. As a result, many points would be removed during the filtering. Figure 8C shows how the removal process affects the overall data coverage. The plot representing line 4E from T tank farm shows that over half of the data are removed. The S tank farm line 2N, on the other hand, shows that less than 5% of the data have been removed. The amount of data removed and general data quality directly affects the inversion process.

Figures A-9 through A-15 in Appendix A show the results of two-dimensional inversion of the surface resistivity data. In addition to the pre-leak inversion, these plots show the results of post-leak and direct differencing between post and pre-leak to highlight the effect of the differences between the two different data sets. Differencing was accomplished by directly subtracting the pre-leak value from the post-leak value through the Surfer[4] contouring software. The two-dimensional inversion results show that a few of the lines see a significant change (decrease in resistivity) due to the leak, whereas others do not. This could be due to the dimensionality of the problem. Since the movement of the plume is definitely three-dimensional, the two-dimensional inversion may be an inadequate methodology for evaluation of the leak. However, each pre- and post-leak inversion result shows a conductive region below the level of the tanks.

After two-dimensional inversion, the data were prepared for three-dimensional inversion with EarthImager3D.[5] To accomplish the three-dimensional inversion, every electrode was geo-referenced in Hanford State Plane coordinates, which allowed an absolute placement of each HRR line within the inversion algorithm. In addition, to reduce processing requirements, the data were decimated such that only those electrodes that fell on a 6-meter spacing were incorporated into the model. Resistivity data were actually collected on a 3-meter spacing. The end results would allow the evaluation of the larger spacings proposed for future SGE work in the B, C, and U tank farms.

---

[4] Surfer and Surfer8 are registered trademarks of Golden Software, Golden, Colorado.

[5] EarthImager2D and EarthImager3D are trademarks of Advanced Geosciences, Inc., Austin, Texas.

Figure 8. Data Filtering for S and T Tank Farms.

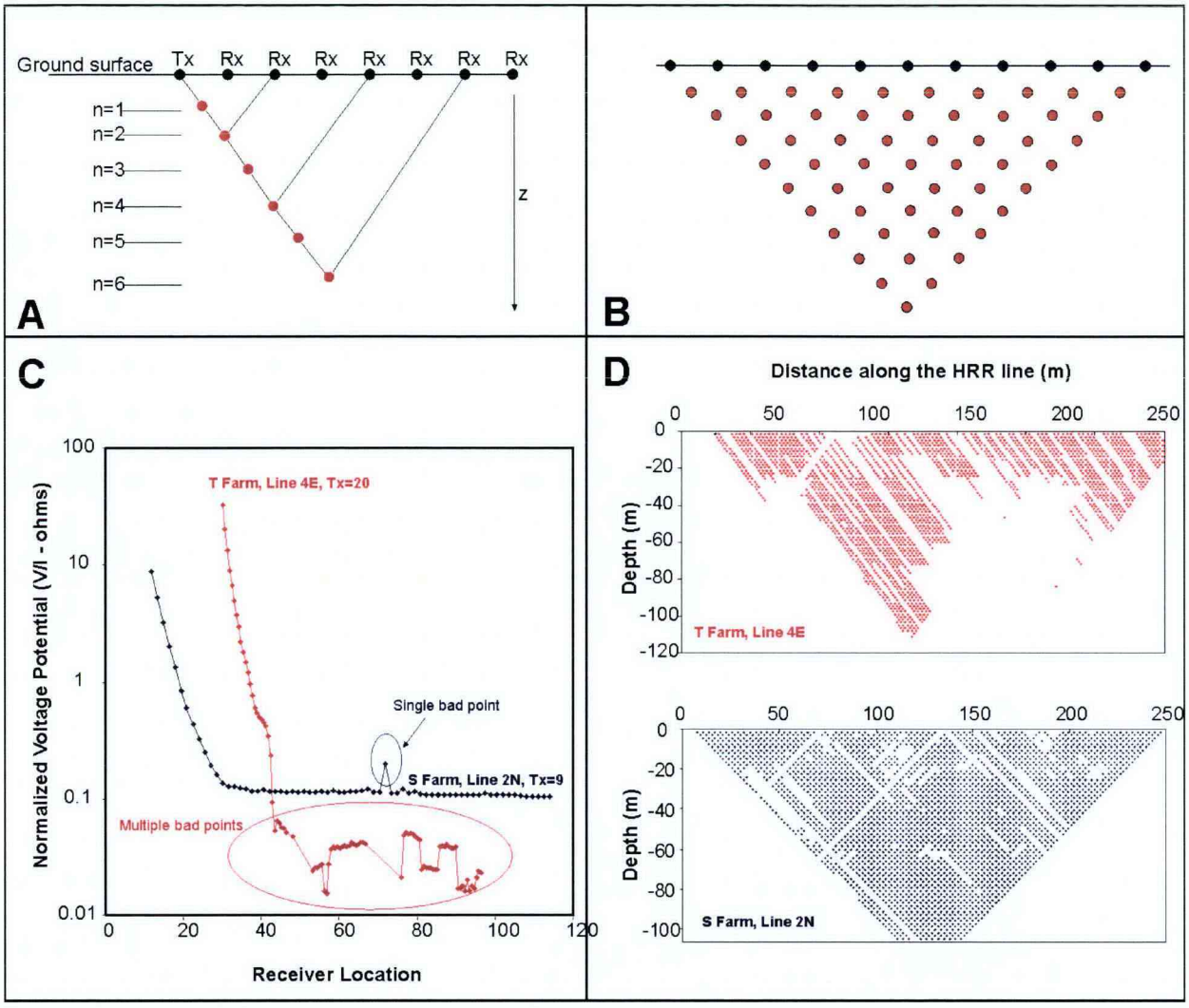

Figures 9 through 11 show the results of the resistivity inversion for the pre-leak survey. Figure 9 is a plan view of the resistivity, showing only the lower end of the resistivity spectrum. The smallest resistivity values are associated with the largest salt concentration or moisture content, and therefore, are generally small in size. From previous experience at the BC cribs and trenches site and T tank farm, the resistivity of the background sandy Hanford formation is in the range of 500–2500 ohm-meters. These high resistivity values are due to low moisture content, natural mineralization and inorganic concentrations, and generally coarse-grained soils.

The resistivity anomaly in Figure 9A is shown at the 1–2 ohm-meter level; Figure 9B shows an anomaly from 1–5 ohm-meters; Figure 9C shows both anomalies combined. The results of the inversion show that the more conductive subsurface is located near tanks S-101, S-102, S-104, and S-105. The results also show a relatively shallow resistivity gradient (Δresistivity/Δdistance).

Figure 9. Plan View of Pre-Leak Three-Dimensional Surface Inversion Results A) 1-2 ohm-meters; B) 1–5 ohm-meters; C) Combination of both resistivity levels.

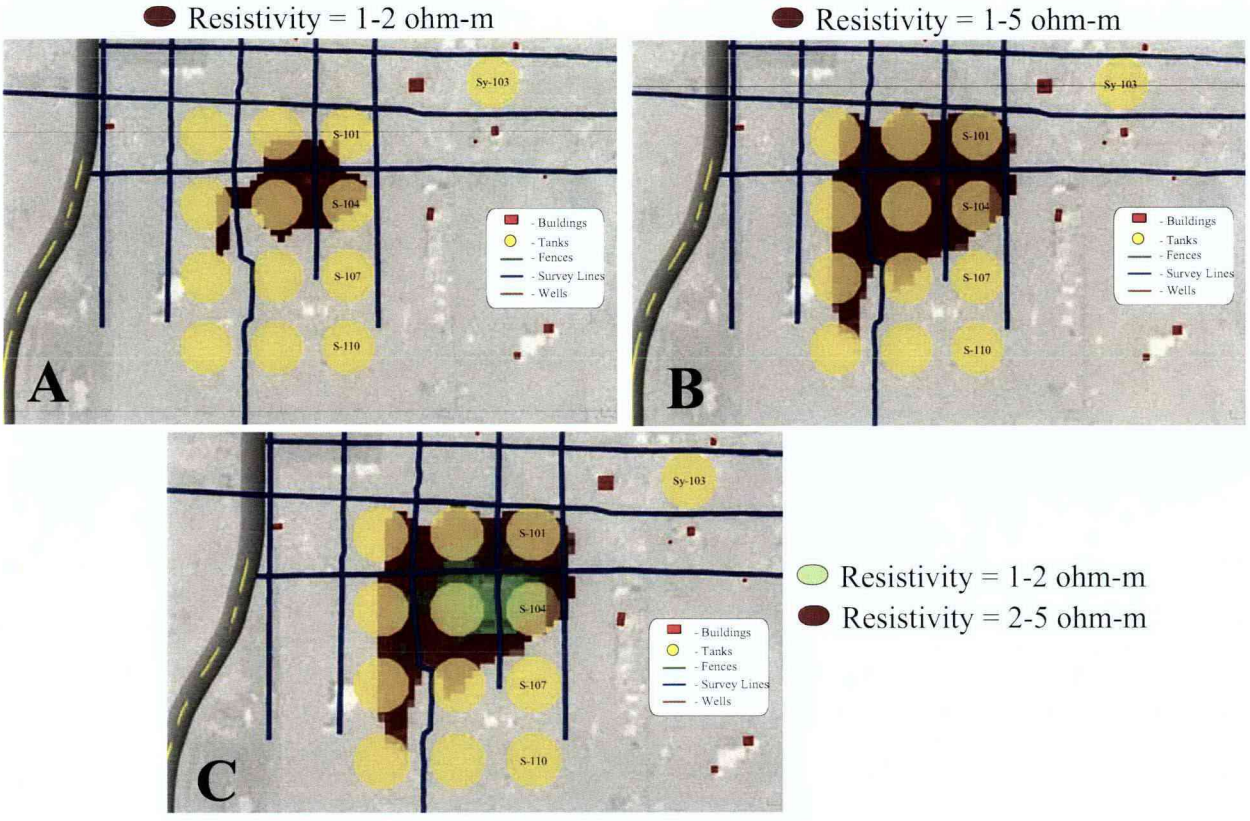

Figure 10 shows the same results of the pre-leak resistivity inversion from a side view. Figure 10A is a view of the resistivity plume at the 1–2 ohm-meter and 2–5 ohm-meter values looking east at tanks S-101, S-104, S-107, and S-110. The lowest resistivity values appear to be associated with tank S-104. Additionally, it appears that the low resistivity value did not reach the water table, located at approximately 70 meters below ground surface (at an elevation of approximately 132 meters above mean sea level). The view of the resistivity plume from the north in Figure 10B also confirms the origin of the resistivity low.

Figure 10. Side View of Pre-Leak Three-Dimensional Surface Inversion Results A) Looking east at resistivity levels of 1–2 ohm-meters (small plume) and 2–5 ohm-meters (large plume); B) Looking north at resistivity levels of 1–2 ohm-meters and 2-5 ohm-meters.

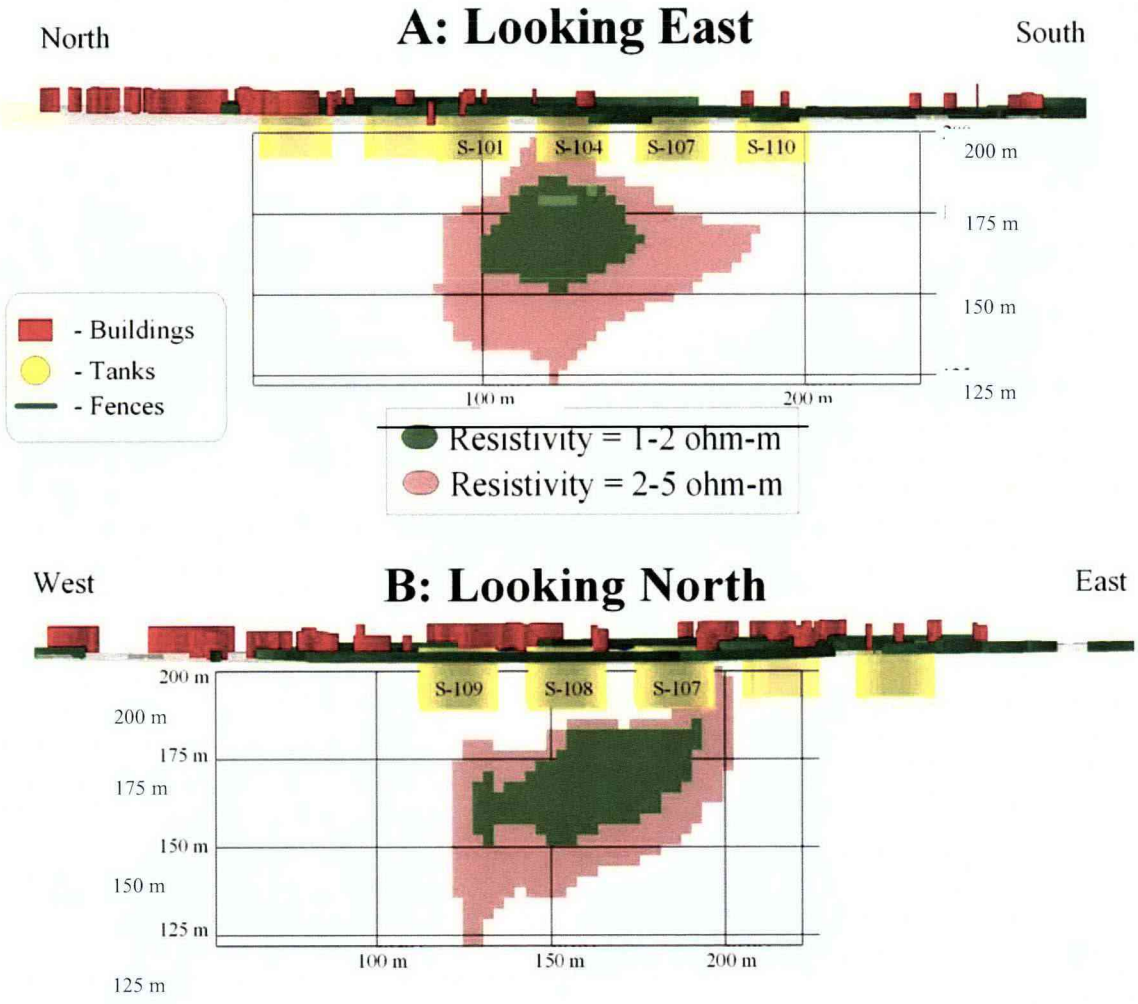

Figure 11 shows a three-dimensional view, looking from the southwest towards the northeast. The same resistivity levels are presented in Figures 9 and 10 and shown in Figure 11; 1-2 ohm-meters and 1–5 ohm-meters.

Figure 11. Three-Dimensional View of Pre-Leak Surface Inversion Results.

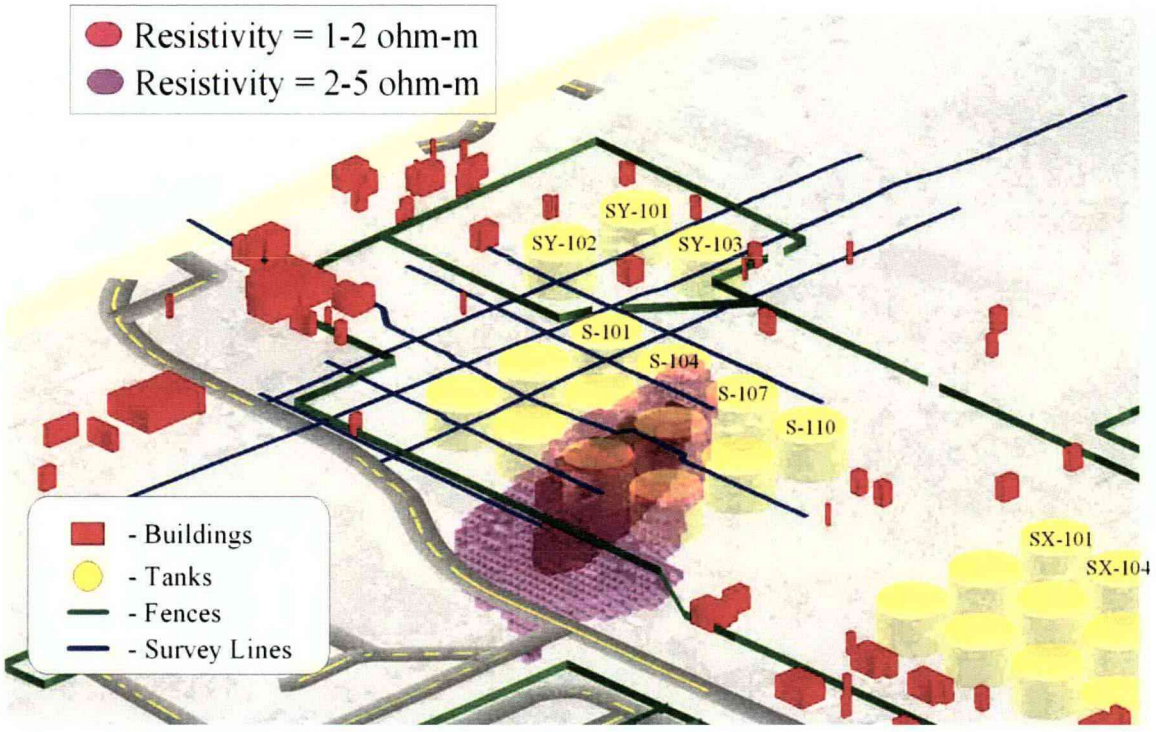

Figure 12 shows the results of the post-leak resistivity survey. Figure 12A shows the plan view of the inversion results with two plume representations, one at 1–2 ohm-meters and the other at 2–5 ohm-meters. This plot can be directly compared to Figure 9C. Figure 12B shows the post-leak resistivity inversion viewed from the side looking north, which is directly comparable to Figure 10B. Figure 12C shows the three-dimensional representation of the resistivity inversion and is comparable to Figure 11.

For a direct comparison, Figure 13 overlays the results of the pre- and post-leak inversion results within the same view. The resistivity plume is for both time periods and is represented at 1-2 ohm-meters and demonstrates how the plume changed after approximately 13,000 gallons of conductive fluid was injected into the subsurface. The plan view in Figure 13A shows that the plume is more northeast, close to the location of well 40-02-10 (the leak injection well). It is reasonable to assume, therefore, that the resistivity changes are directly resulting from an increase in moisture and salt content after injection. The other two views also demonstrate how the leak migrated through the subsurface.

Figure 12. Views of Post-Leak Surface Inversion Results. A) Plan View for resistivity values of 1–2 ohm-meters and 2–5 ohm-meters; B) Side view for resistivity values of 1-2 ohm-meters and 2–5 ohm-meters; C) Three-Dimensional View for resistivity values of 1–2 ohm-meters and 2–5 ohm-meters.

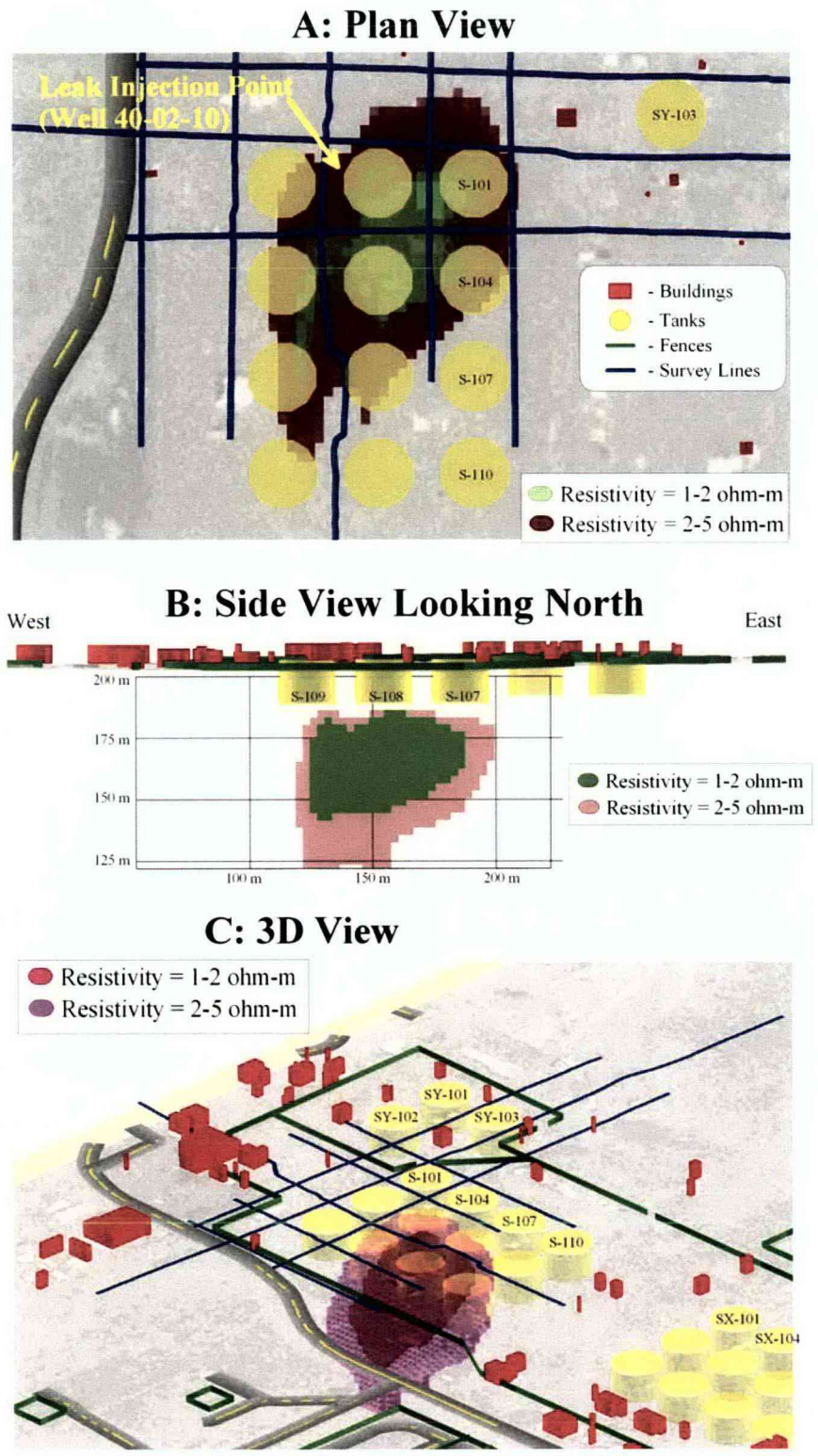

Figure 13. Views of Pre- and Post-Leak Surface Inversion Results for the 1-2 ohm-meter Level. A) Plan View; B) Side View; C) Three-Dimensional View.

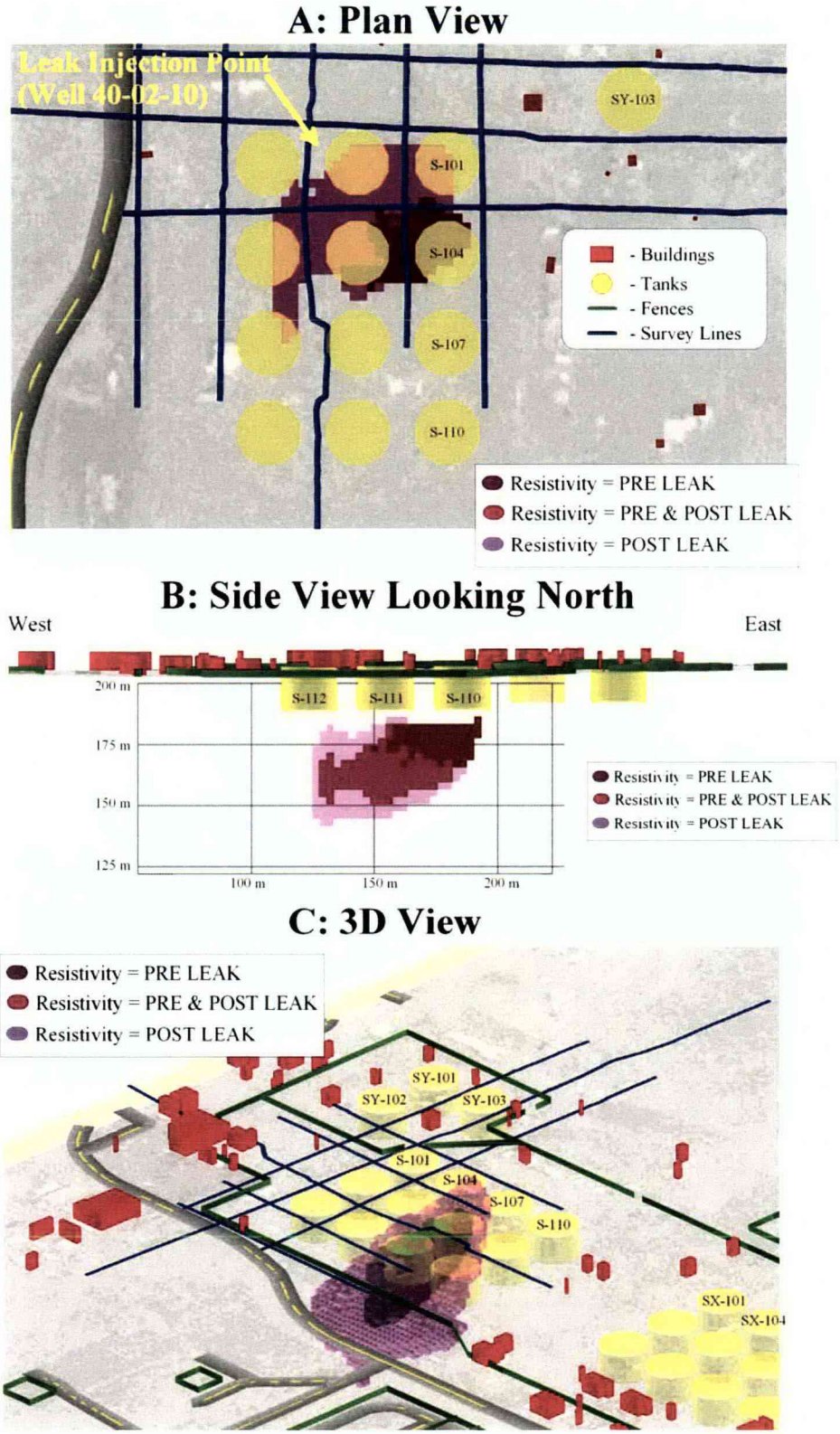

Figure 14 shows the difference between the pre- and post-leak inversion results. The figure shows an opaque plume that highlights areas that have the largest decrease in resistivity as expressed in percentage. Figure 14A shows the regions where the resistivity of the subsurface decreased between -80% to -55% as a result of conductive fluid entering the vadose zone. An 80% decrease in resistivity is the largest observed in the surface data. Figure 14B shows the areas of highest change from -80% to -70%, which is markedly smaller than Figure 14A. These zones of decreasing resistivity highlight the migration of the injected fluid from well 40-02-10. There also appears to be significant travel southward to tanks S-111 and S-112. The reliability of data may be slightly lower in this area due to the lack of orthogonal lines in the southern portion of the domain. This is especially noticeable since the decrease in resistivity is associated with a single line, line 3E. Future surveys should take care in including a sufficient number of orthogonal lines to validate observations.

Figure 14. Percent Decrease in Resistivity from Post- to Pre-Leak Results,
A) Opaque plume showing areas of decrease between -80% to -55%;
B) Opaque plume showing areas of decrease between -80% to -70%.

A: Resistivity Percent Decrease -80% to -55%

B: Resistivity Percent Decrease -80% to -70%

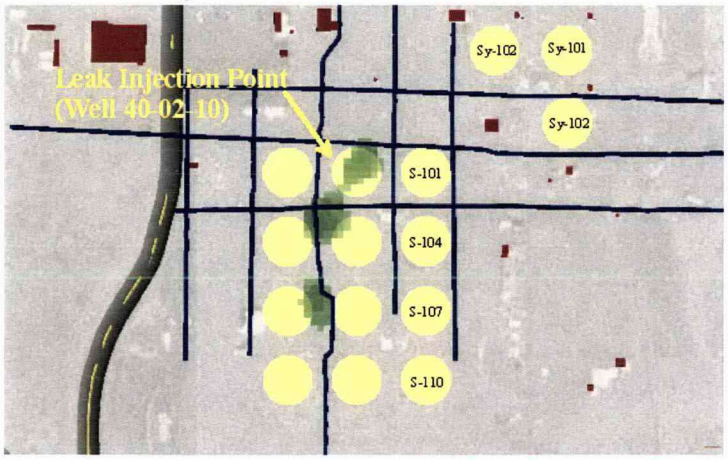

Figures 9 through 14 qualitatively demonstrate the changes between the pre- and post-leak resistivity surveying. A quantification of the changes in subsurface properties can be seen in Figure 15. This figure was generated as a cumulative distribution function. The x-axis shows matrix (or total cell) volume and the y-axis shows the resistivity value associated with that volume. The usefulness of the graph is comparing pre- and post-leak volumes for a constant resistivity (e.g., 5 ohm-meters). For the pre-leak case, the 5 ohm-meter resistivity level encompassed 138,780 cubic meters of soil, including the pore volume. After injection, the 5 ohm-meter resistivity level increased to a volume of 202,500 cubic meters. The total change in matrix volume from pre- to post-leak is 63,720 cubic meters (16.8 x 10^6 gallons).

Figure 15. Matrix Volume Calculations for Pre- and Post-Leak Resistivity Inversion.

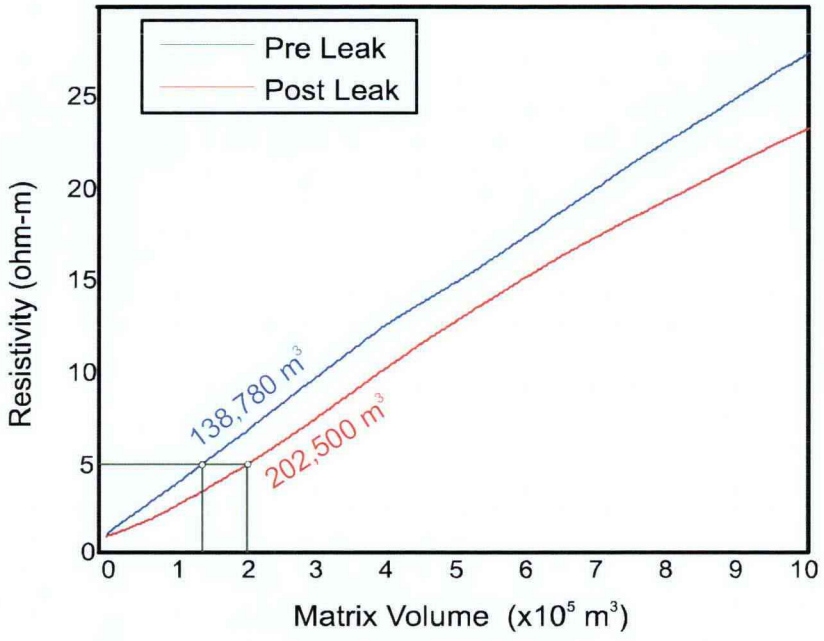

4.2 WELL-TO-WELL INVERSION

The WTW inversion involved the use of drywells as current transmission and voltage potential measurement electrodes. The background and theory for the WTW inversion can be found in RPP-RPT-28955.

For the S tank farm leak injection test, a total of 42 wells were used for the data acquisition phase, which included both drywells and groundwater wells. For this particular study, only the drywells in the vicinity of the tanks were used based on: 1) the T tank farm WTW inversion produced results that were less amenable to vadose zone plume interpretation when combining groundwater and vadose wells, and 2) the spacing for the groundwater wells was sufficiently large as to produce results with extremely low resolution. Figure 16 shows the 31 vadose zone wells used for WTW inversion for the pre- and post-leak evaluation. The most obvious well omitted from the inversion was the leak injection well, 40-02-10. This well was unavailable for the SGE data acquisition.

Figure 16. Wells Used for the SGE WTW Resistivity Inversion for Pre- and Post-Leak.

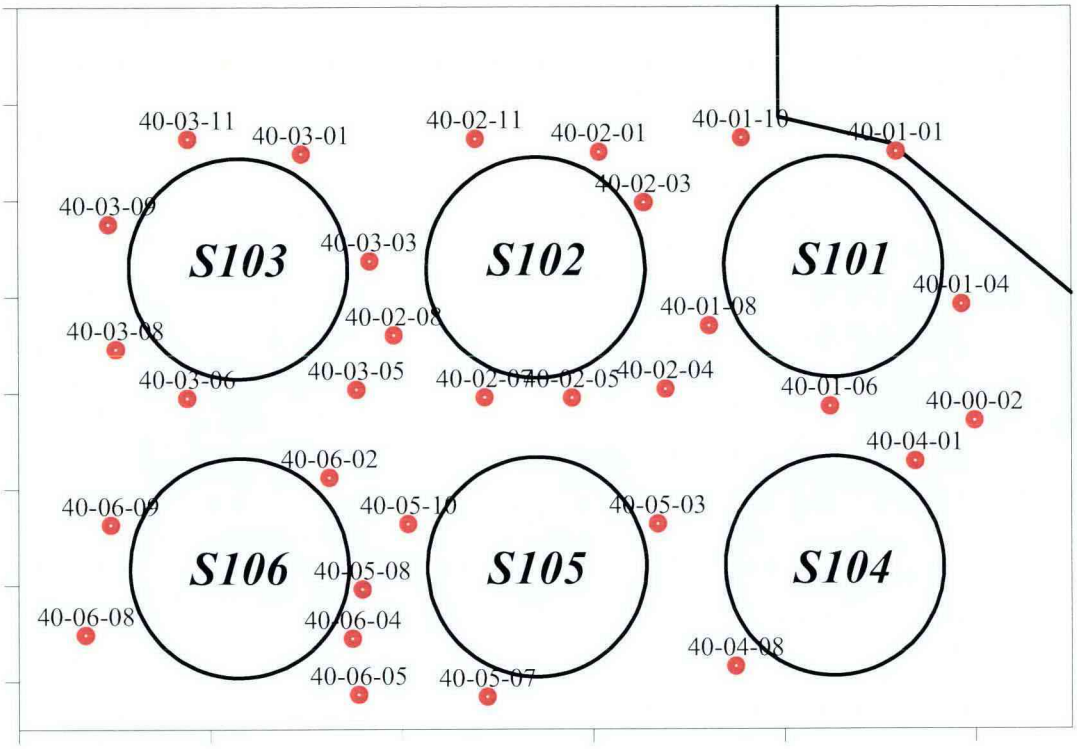

Figure 17 shows the results for the WTW inversion for both pre- and post-leak results. The results are presented at two separate opacity values, 0–15 ohm-meters and 0–20 ohm-meters. Several notable features exist within the figure. First, the data are only presented from a two-dimensional plan perspective. Based on the geometry of the problem, it is not possible to position the resistivity plumes in the vertical (z) dimension without ancillary data (e.g., moisture content, salt content, or other data that can discriminate the electrical resistivity in this dimension). Second, Figure 17A shows that the lowest resistivity values are concentrated beneath tanks S-102 and S-105. This is slightly different than the surface inversion results, which also included tank S-104. The reason for the slight discrepancy is that the resolution and data coverage on the west side of tank S-104 is low. In order to better resolve the issue, more wells (or surface electrodes) are needed in this area. Last, the pre- and post-leak results show a low resistivity anomaly at tank S-107. Unfortunately, there were no wells around this tank that were used in the data acquisition phase. Therefore, the results in the southeast corner of the plot are highly suspect and should be discounted as a processing/plotting anomaly.

Figure 17. WTW Inversion Results for Pre- and Post-Leak Data.

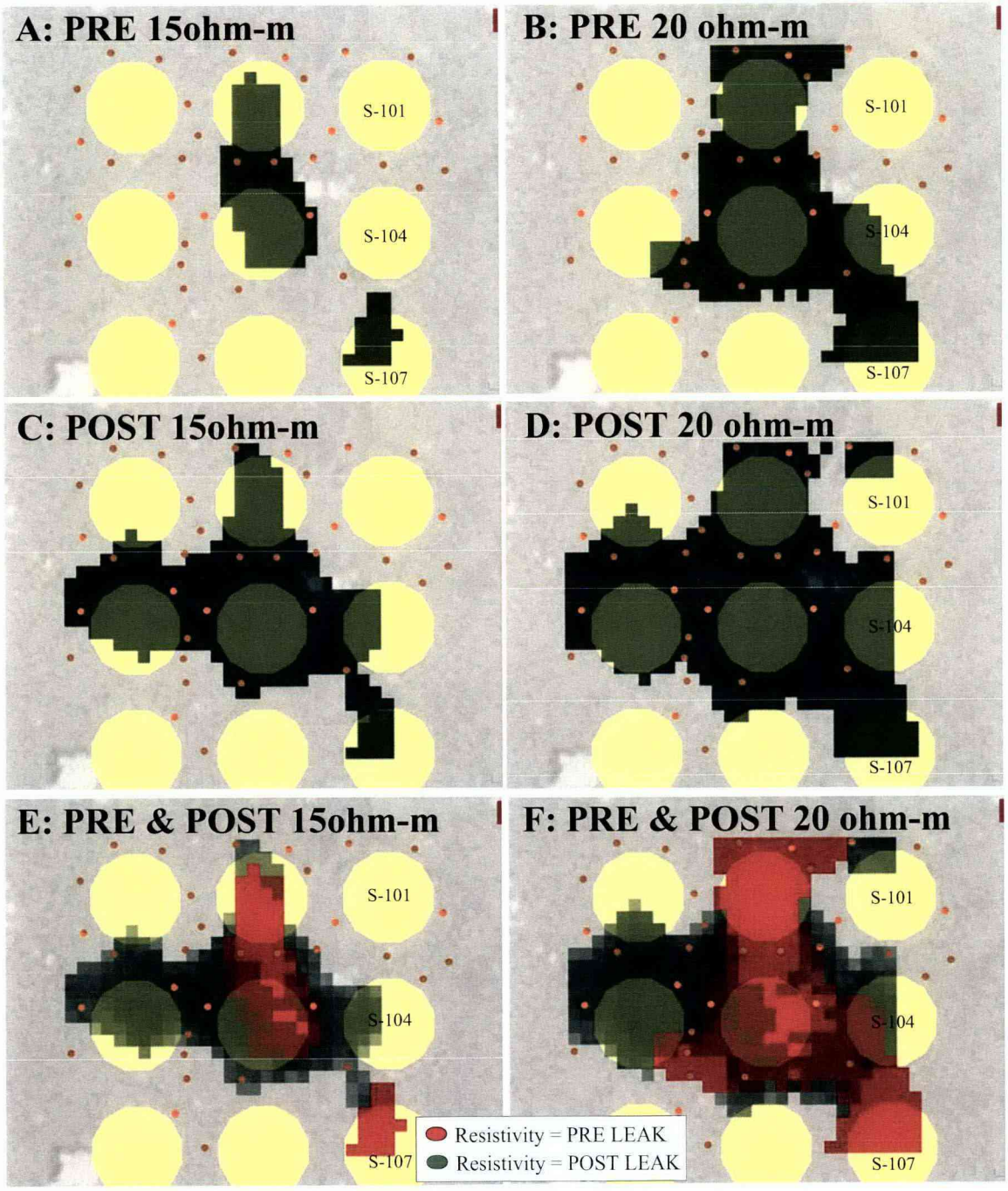

Between the pre- and post-leak injection surveying with SGE, the HRR-LDM system was connected to a subset of wells around tank S-102 for calibration. The system is connected to 15 wells, 8 surface electrodes, and 2 tanks (i.e., S-102 and S-103). The system measures the voltage potential and current injection on almost every combination with a 17-minute cycle. To understand the flow dynamics of the fluid migration between the pre- and post-leak end points and to demonstrate the power of the SGE functionality, the LDM well data were inverted using the EarthImager3D code. Inversion occurred by first inverting the pre-leak data, which is used as a base case. For subsequent mid-leak inversions, the pre-leak resistivity data were used as the starting estimate. Typically, the starting estimate for each inversion is a constant throughout the entire domain, and is established by calculating the average apparent resistivity. By using the pre-leak results as an *a priori* starting model, the inversions finish faster and are more consistent with each other.

Figure 18 shows the inversion results for the 15-well LDM subset. The wells cover a very limited area, and focus mainly on tank S-102. The figure shows the progression of the resistivity change after each leak has finished, and the data are presented as percent change from baseline conditions. The cool colors (blues and purples) represent a decrease in resistivity, which is expected during an injection of a conductive solution. At the early stages of the leak injection test, through leak 5, the decrease in resistivity is confined to a relatively small zone around the leak injection well 40-02-10. Leaks 6 through 9 begin to show a marked decrease to the south of tank S-102. Finally, immediately after leak 10, the injection appears to have migrated to cover the whole western side of tank S-102.

When comparing leak 10 LDM WTW results with the post-leak SGE, a similarity is noticed. Both data sets show the plume moving west and south (and a little north) from the injection well. The two results are not exact, however, and must be viewed qualitatively. The reason for the differences is that the LDM data set includes the injection well. Additionally, the LDM results show a very narrow view of the S tank farm relative to the SGE results.

At first glance, the WTW and surface resistivity inversion results show highly disparate results. Figure 19 was constructed to allow a direct comparison between the two data sets. The figure shows both pre- and post-leak data for WTW (represented by an opacity of 0-14 ohm-meters) and surface (represented by an opacity of 0–1.5 ohm-meters). The results do not overlap each other perfectly. They do, however, show similar features and overlap by almost 60% for the pre-leak case and 66% for the post-leak case.

Figure 18. WTW Inversion Results for LDM Data Showing Percent Change from Baseline (Pre-Leak) Conditions.

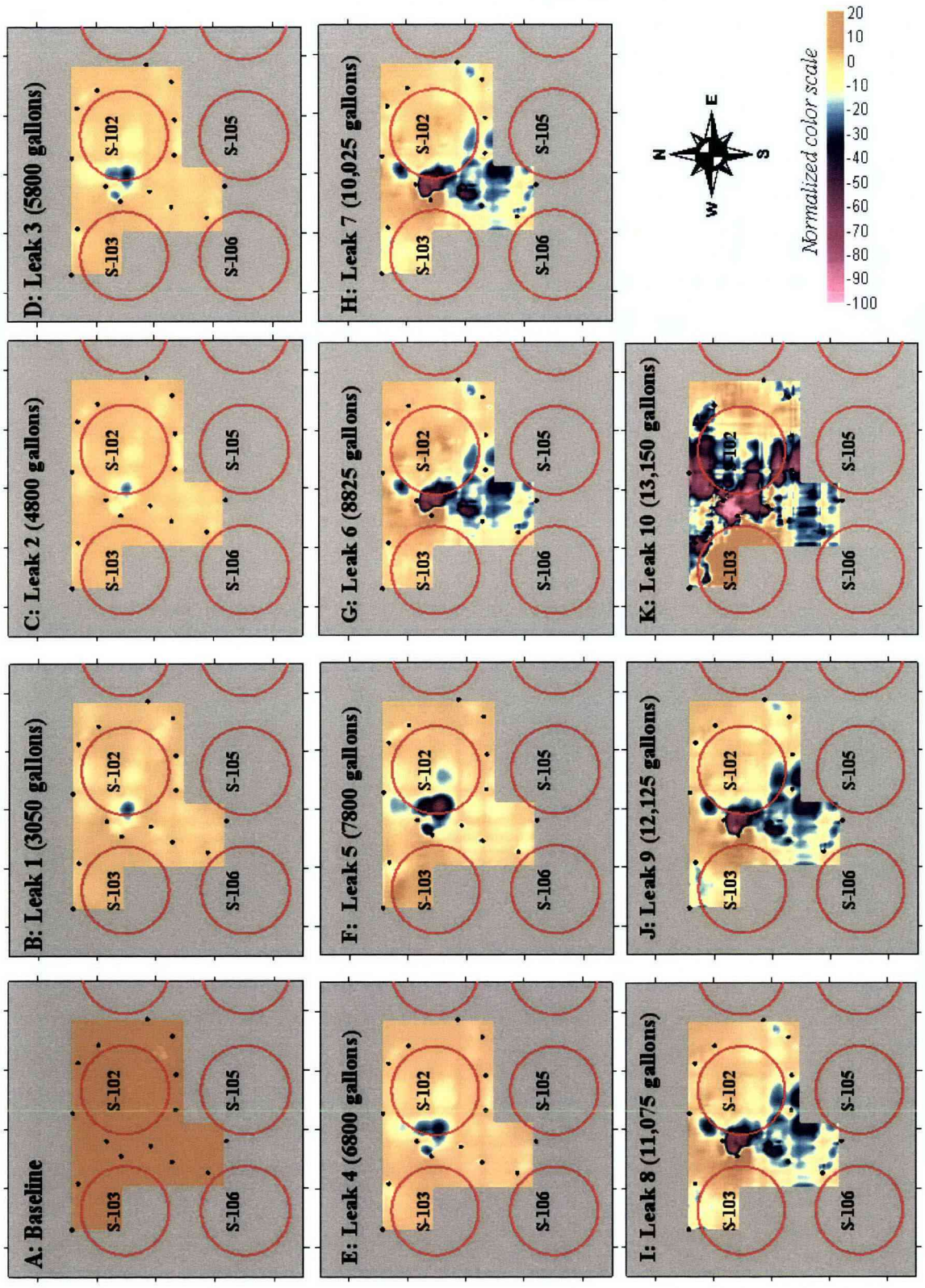

Figure 19. Direct Comparison of WTW Inversion with Surface Inversion, with WTW Opacity (red) of 1–14 ohm-meters and Surface Opacity (green) of 1–1.5 ohm-meters.

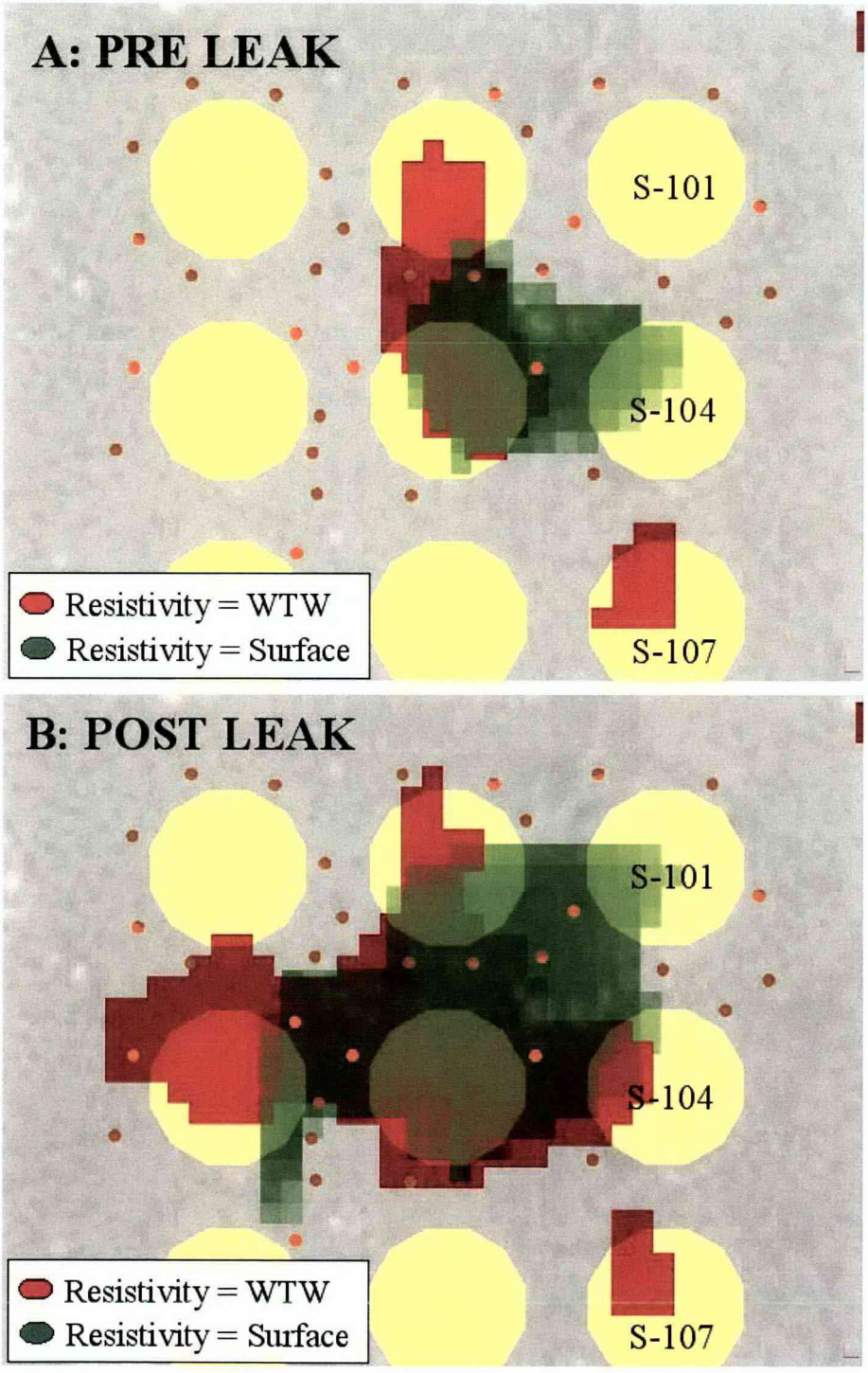

4.3 COUPLED WELL-TO-WELL AND SURFACE INVERSION

The last set of inversion trials included a combination data set that combined both WTW and surface data into one file each for pre- and post-leak snapshots. It did not include, however, a WTS data set, where current transmission was conducted on a well and voltage potential measured on the surface (and vise versa). The results for the combination inversion data set are shown in Figure 20 for both pre- and post-leak results, where the resistivity plume is presented at the 1–5 ohm-meter value. The pre-leak data shows a resistivity plume that is elongated in the north-to-south direction and extending primarily beneath tanks S-105 and S-102. The post-leak results show an increase in coverage of the resistivity plume after injection, extending in all directions except to the northwest.

Figure 20. Combination Data Set of WTW and Surface Inversion, with Opacity (red) of 1-5 ohm-meters showing A) Pre-Leak Results, B) Post-Leak Results, and C) Pre- and Post-Leak Results.

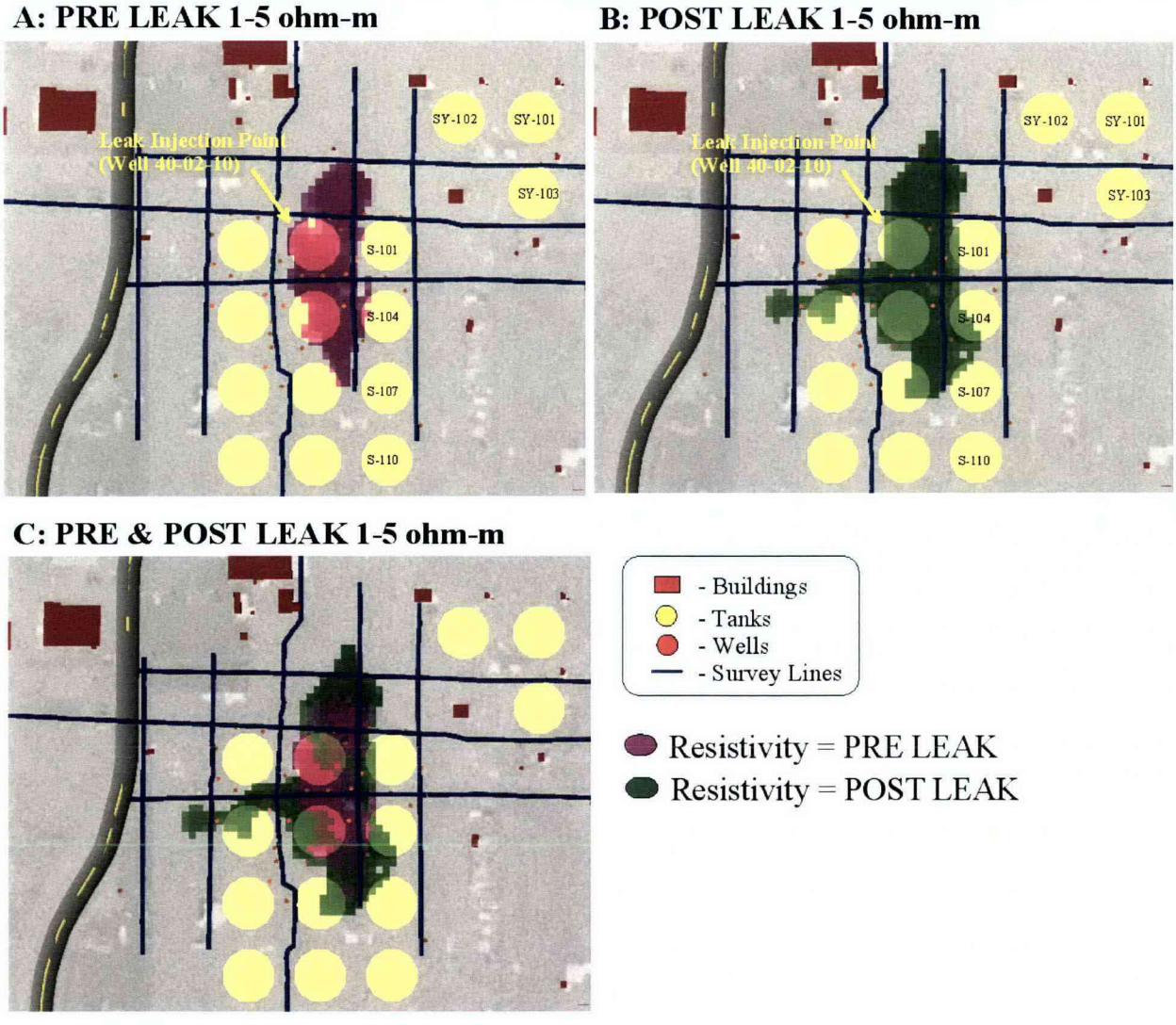

The results of the combination inversion resemble the WTW inversion results more than the surface inversion results in general shape. Figure 21 highlights all three plumes by outlining the extent of each plume in plan view for the pre-leak case. The WTW and combination inversion appear to be elongated in the north-to-south direction, whereas the surface inversion results appear to be more circular. The surface data does, however, influence the actual values of resistivity, where the combination resistivity plume from 1–3.8 ohm-meters are closer to the 1-2.2 ohm-meter values of the surface resistivity data. Figure 21 shows how the resistivity results change with different means of data collection and analysis.

Figure 21. Direct Comparison of Pre-Leak Inversion Results Showing Surface Only Plume Outline at 1–2.2 ohm-meters, WTW Only at 1–16 ohm-meters, and the Combination Data Set at 1–3.8 ohm-meters.

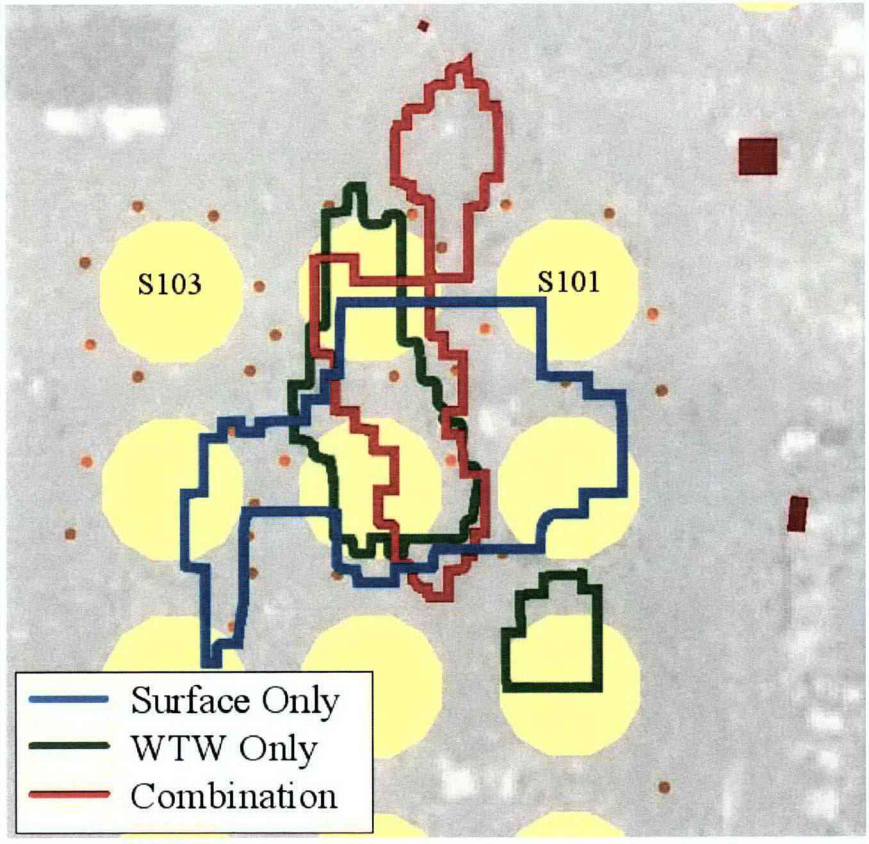

5.0 CONCLUSIONS

Many successes were realized during the S tank farm SGE including the positive identification and correlation of historical leaks beneath tank S-104, positive identification and correlation of the recent leak injection, and the high correlation between surface and WTW inversion results. A greater confidence can now be given to the results obtained at the T tank farm (RPP-RPT-28955).

5.1 HISTORICAL LEAK ASSESSMENT – PRE-LEAK

The results for the pre-leak survey show a resistivity low that appeared to originate from tank S-104. This resistivity low also appeared beneath tanks S-105 to the west and S-102 to the northwest in the 1–2 ohm-meter resistivity level. The plume extended under many other tanks, particularly to the south, for the 2–5 ohm-meter resistivity level. Historical fluid releases associated with tank S-104 correlate with some portion of the interpreted resistivity plume. The lowest resistivity value (1–2 ohm-meters) does not appear to have reached the water table. Other extensions of the plume may also coincide with pipe leaks.

5.2 LEAK INJECTION ASSESSMENT – POST-LEAK

Surface Data Only

The post-leak surface resistivity results show a decrease in resistivity extending from the leak injection location at well 40-02-10 (northwest quadrant of tank S-102) and moving primarily southward on the west side of S-102. Some of the plume also appears to have migrated northeast of S-102. Percent difference results from pre- to post-leak, show a significant change near tank S-111. This change is attributed to limitations in data acquisition and processing, and is not interpreted to represent a plume response.

Well-to-Well Data Only

WTW inversion showed a general decrease in resistivity between pre- and post-leak data sets. The low resistivity values increased in coverage area with the introduction of the leak injection fluid, while the areas of higher resistivity values decreased. The WTW and surface inversion results were compared qualitatively by overlapping similar resistivity plumes, and quantitatively by calculating coincident coverage areas of the plumes. Qualitative comparison of the electrode specific results all show a plume beneath tanks S-102 and S-105.

Comparison of WTW Data with Surface Data

A quantitative comparison shows that the WTW and surface inversion results generally differ by an order of magnitude. Additionally, resistivity plume representation from the WTW and surface data show an overlap of almost 60% for the pre-leak and 66% for the post-leak. The T tank farm SGE results showed similar features, where the WTW and surface inversion

results did not match perfectly. The differences are most likely due to the differences in resolution, coverage area, and electrode geometry.

Combination of WTW and Surface Data Inversion

WTW and surface data were combined into one file each for the pre-leak and post-leak injection tests. The combination inversion results show that the WTW data have a strong influence on the overall shape of the results and the surface data have a strong influence on the resistivity values. Although not readily apparent from the S tank farm SGE investigations, the combination data set may be more advantageous in areas where surface data are of low resolution. An example is the T tank farm SGE, where in-farm coverage of surface resistivity was of poor quality and WTW out-farm coverage was of poor resolution. The combination of out-farm surface data and in-farm WTW could possibly have provided limited depth information within the T tank farm.

HRR-LDM Data Using SGE Processing

The LDM WTW data provided a unique opportunity to see how the leak progressed after each individual leak test. The inversion shows how the leak progressed from a mass very near the well to something that was much larger at the end of the test. Because there were so few measurements for the LDM inversion, the match between the SGE post-leak inversion and LDM leak 10 is not perfect. However, it does demonstrate the usefulness of the SGE processing methodology applied to LDM data.

6.0 ISSUES AND CONCERNS ASSOCIATED WITH INTERPRETATION

Temporary electrodes were used for the pre-leak survey, where the electrodes were removed immediately after the survey was complete. Permanent electrodes were used for the post-leak survey, which remain in place to date (August 21, 2006). It is unknown the exact impact of these different electrode sets on the data quality and data comparison. However, areas with small changes in resistivity would have the most impact. Areas of small changes generally occurred on the periphery of the tank farm. Permanent electrodes will certainly decrease noise and increase the sensitivity to smaller leaks that may occur in the future.

Discussions on the calibration of SGE data with petrophysical relations derived from laboratory analyses have begun. The petrophysical relations would show, for example, the response of electrical resistivity to increasing water content and salt (e.g., sodium nitrate) content. Although these relations have not been developed yet, HGI will soon start making these measurements for Hanford-specific (and tank farm-specific) soils and contaminants.

There are concerns over false positives and false negatives. An example of a potential false positive is seen in Figure 17 near tank S-107. The low resistivity values found here are suspect. The low resistivity does not match hydrologic expectations from known leak locations. Additionally, the area has low coverage in the WTW data, and therefore, has a low sensitivity to any value placed in the region (i.e., it could accommodate almost any value without affecting the

model results to any great degree). However, without explicit testing of the soil, it is unknown if a zone of high moisture or salt content resides in one particular area. The different geometries can help confirm suspected areas, but a true test would require core sampling.

To help establish confidence in evaluating areas of low resistivity, the following criteria should be confirmed.

- Do the results match hydrologic expectations correlating to waste disposal areas?
- Can the results be verified through published core sampling data?
- Can the results be verified through a different geometric configuration of SGE?
- Are the low resistivity areas continuous over broad areas?
- For time series snapshots (e.g., pre- to post-leak), do the results match hydrologic expectations?

Comparisons are often made to the other characterization methods employed at the tank farms such as spectral gamma logging. This comparison is not endorsed on many levels. First, the scales of measurement between the two systems are highly disparate. The spectral gamma logs a drywell in close proximity to the well. SGE, on the other hand, obtains large scale volumetric averages covering areas the size of tank farms. The scale increases for surface resistivity inversion with depth, and increases for WTW inversion at larger separations. Second, the contaminant of interest for each method (inorganics for SGE and gamma-emitting radionuclide for spectral gamma) moves through the vadose zone under different mechanisms. Inorganics, especially nitrate, are transported primarily under advection with little to no retardation. The nitrate plume will be relatively large. Most gamma-emitting radionuclides have large retardation coefficients and are transported more slowly. These radionuclide plumes are expected to be much smaller than the inorganic plumes.

7.0 RECOMMENDATIONS

Several recommendations are suggested to improve the data acquisition, data quality, and data coverage of future SGE efforts at the Hanford Site tank farms.

- The success of SGE at both S and T tank farms in terms of the ability to locate and map areas of low resistivity lends credibility to the method for identifying historical leaks. It is recommended that all other farms be imaged with SGE, including a full-scale characterization of S tank farm.

- Develop a plan and strategy to iteratively develop sufficient confidence in the SGE results through confirmatory sampling, verification, and testing to support ongoing program needs to provide technically defensible estimates of contamination currently in the vadose zone along with ongoing monitoring.

- Install permanent surface electrodes within the farm to reduce time and costs for SGE deployment. This idea was first initiated for S tank farm and the strategy should continue to other farms.

- Computational power was limited for both S and T tank farms. It is recommended that the EarthImager3D code be fully parallelized to run on a multi-processor personal computer with extended random access memory.

- LDM resistivity data were evaluated with a processing methodology developed primarily for SGE data. It is recommended that a larger LDM hardware system be developed that can monitor and characterize an entire farm, where SGE-type processing can be performed at pre-determined intervals to ensure that no leaks are occurring during retrieval.

- Vertical resolution is relatively low (compared to lateral resolution) for the surface resistivity data collection and non-existent for WTW resistivity. It is recommended that as many subsurface point electrodes be installed as possible, including electrical resistivity tomography (ERT) arrays that have many point electrodes along a single borehole. The ERT arrays would increase vertical resolution.

8.0 REFERENCES

ARH-2977, 1974, *Report on the Cleanup Activities Following the 241-S Tank Farm Contamination Occurrence at the Hanford Reservation Richland, Washington on November 14, 1973*, Atlantic Richfield Hanford Company, Richland, Washington.

CEES-0320, 2006, *Test Report for the Leak Injection Test at Tank 241-S-102*, Rev. 3, Columbia Energy & Environmental Services, Inc., Richland, Washington.

HNF-4936, 1999, *Subsurface Conditions Description for the S-SX Waste Management Area*, Rev. 0, Lockheed Martin Hanford Company, Richland, Washington.

HNF-EP-0182, 2006, *Waste Tank Summary Report for Month Ending June 30, 2006*, Rev. 219, Lockheed Martin Hanford Corporation, Richland, Washington.

PNNL-15670, 2006, *Hanford Site Groundwater Monitoring for Fiscal Year 2005*, Pacific Northwest National Laboratory, Richland, Washington.

RPP-7884, *Field Investigation Report for Waste Management Area S-SX*, Rev. 0, CH2M HILL Hanford Group, Inc., Richland, Washington.

RPP-30121, 2006, *Tank 241-S-102 High-Resolution Resistivity Leak Detection and Monitoring Testing*, Rev. 0, CH2M HILL Hanford Group, Inc., Richland, Washington.

RPP-RPT-28955, 2006, *Surface Geophysical Exploration of T Tank Farm at the Hanford Site*, Rev. 0, CH2M HILL Hanford Group, Inc., Richland, Washington.

WHC-MR-0227, 1991, *Tank Wastes Discharged Directly to the Soil at the Hanford Site*, Rev. 0, Westinghouse Hanford Company, Richland, Washington.

APPENDIX A

S TANK FARM SURFACE GEOPHYSICAL EXPLORATION FIGURES

LIST OF FIGURES

High Resolution Resistivity at 241-S Farm - Line 1E

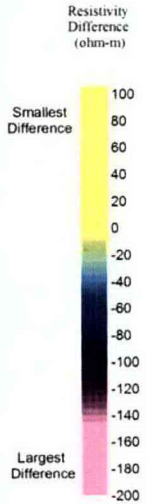

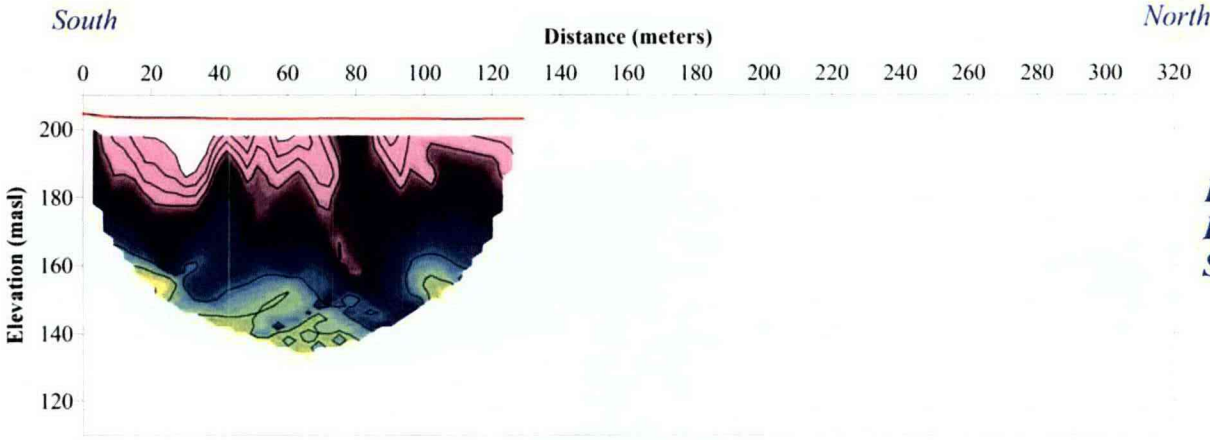

Filtered Differenced Section

Map of Survey Lines

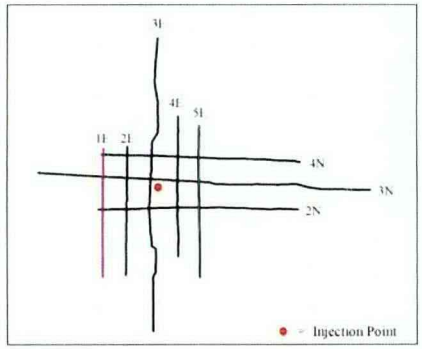

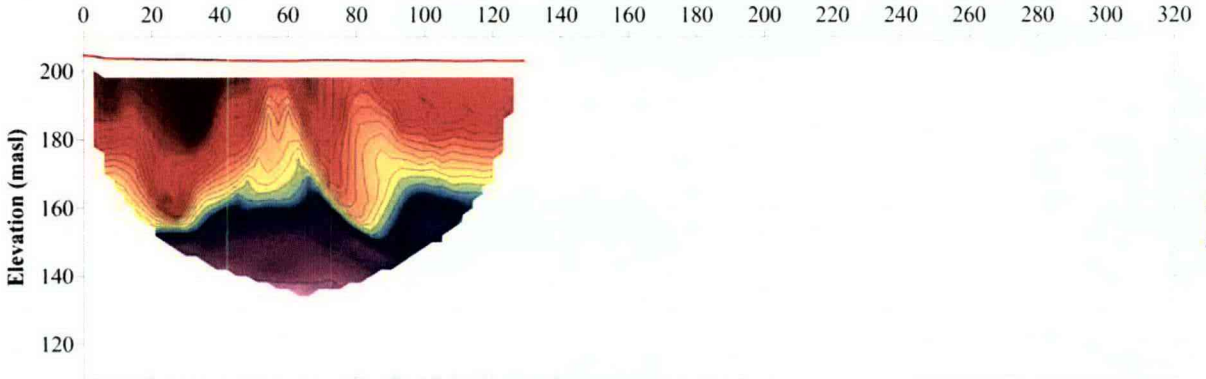

Filtered Pre-Leak Section

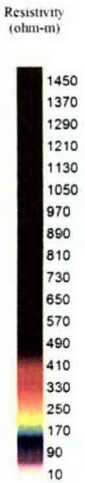

EQUIPMENT

Method: HRR
Rx/Tx: Advanced Geosciences Super Sting R8
Array: Pole-Pole
Spacing: 3 meter
Electrodes: 18" Stainless Steel

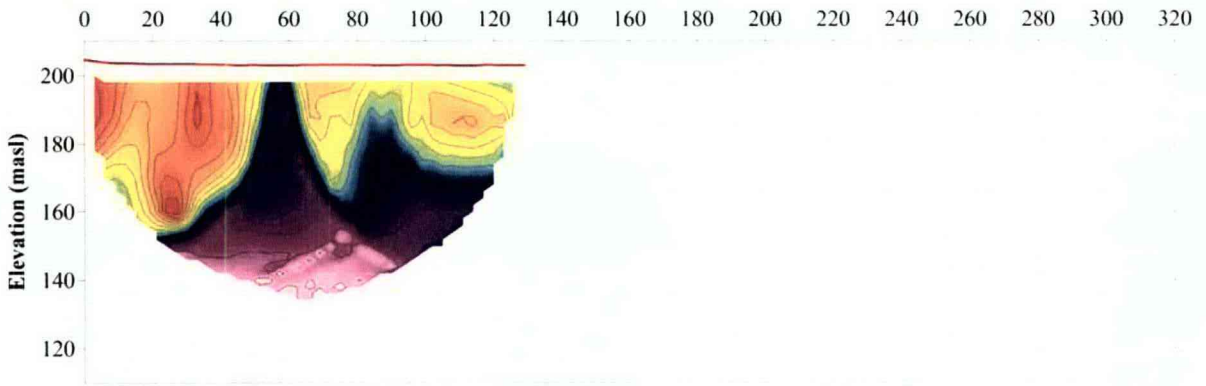

Filtered Post-Leak Section

Scale: 1 in = 30 ft
Vertical Exaggeration.: 1:1

0 15 30 45 60 75 90 105

Resistivity

CHG
241-S Farm
Hanford, WA

Date: Aug 2006 ***Figure: A -***

High Resolution Resistivity at 241-S Farm - Line 2E

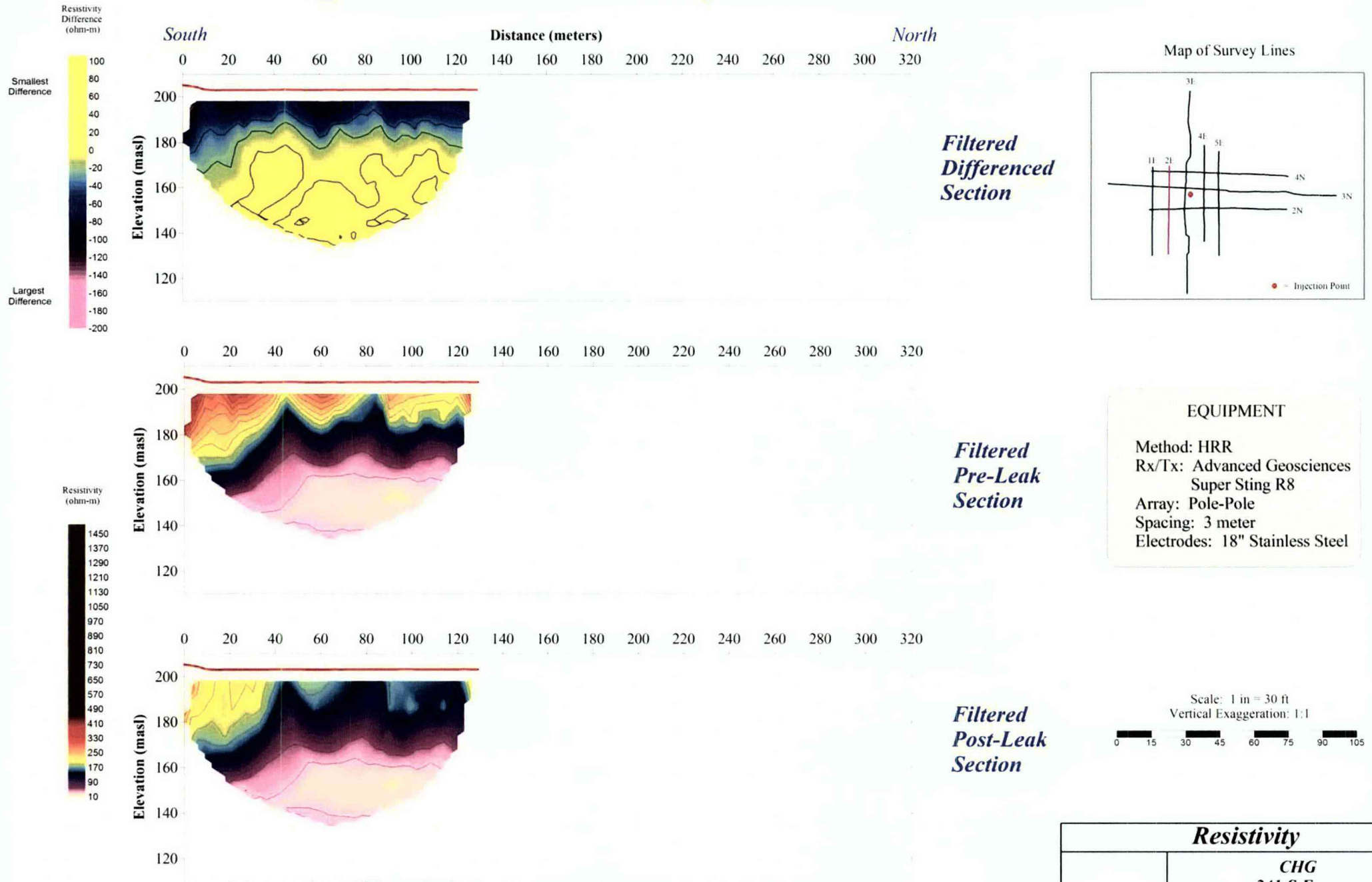

Map of Survey Lines

EQUIPMENT

Method: HRR
Rx/Tx: Advanced Geosciences Super Sting R8
Array: Pole-Pole
Spacing: 3 meter
Electrodes: 18" Stainless Steel

Scale: 1 in = 30 ft
Vertical Exaggeration: 1:1

0 15 30 45 60 75 90 105

Resistivity

CHG
241-S Farm
Hanford, WA

Date: Aug 2006 Figure: A -

High Resolution Resistivity at 241-S Farm - Line 2N

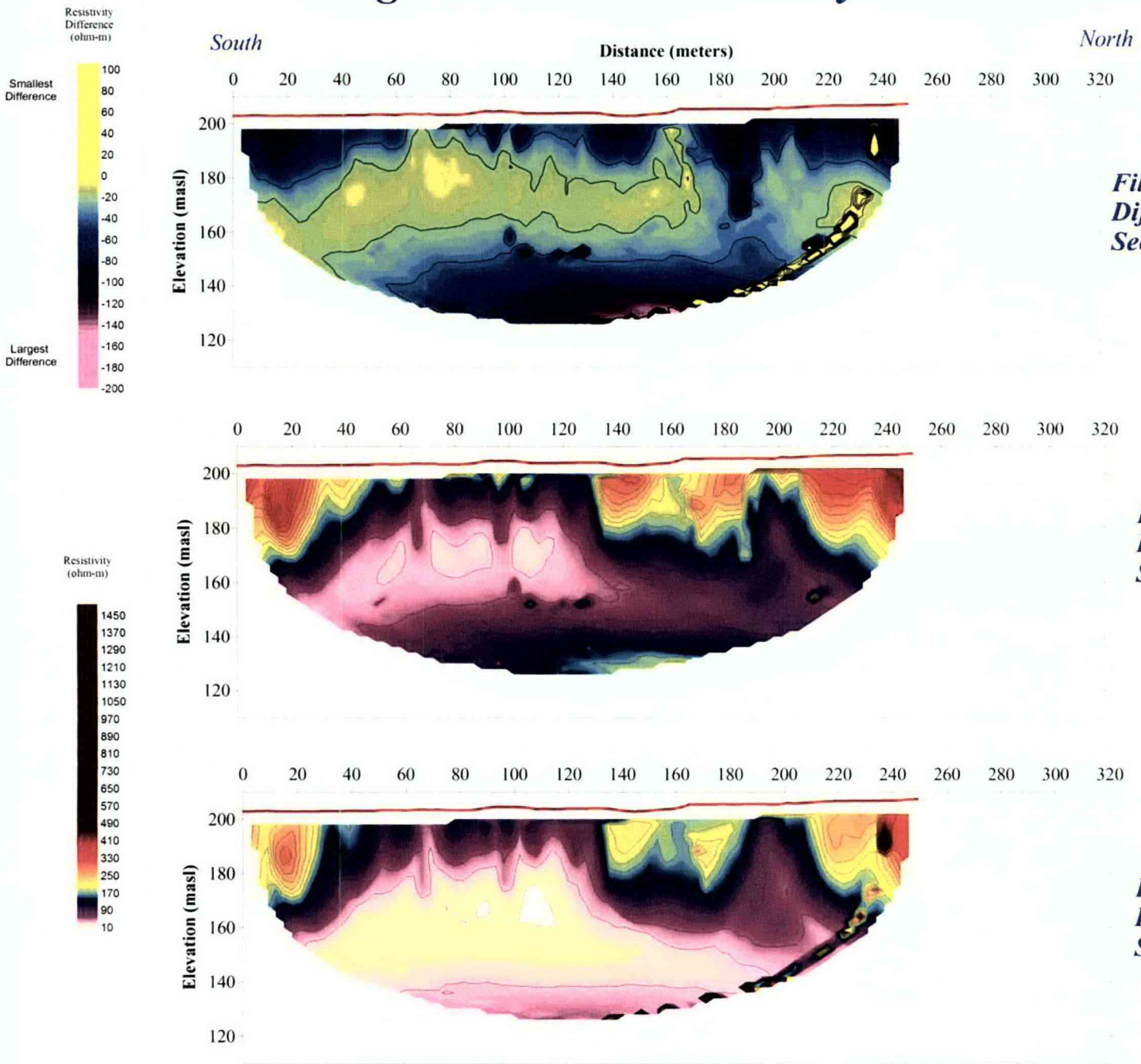

Map of Survey Lines

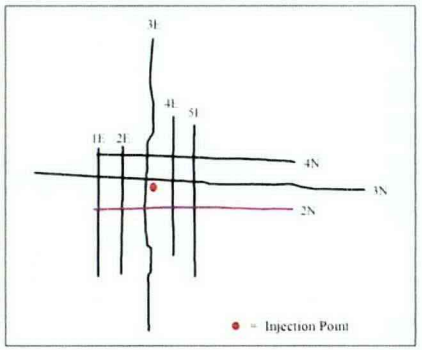

EQUIPMENT

Method: HRR
Rx/Tx: Advanced Geosciences Super Sting R8
Array: Pole-Pole
Spacing: 3 meter
Electrodes: 18" Stainless Steel

Scale: 1 in = 30 ft
Vertical Exaggeration: 1:1

0 15 30 45 60 75 90 105

Resistivity

CHG
241-S Farm
Hanford, WA

Date: Aug 2006 Figure: A-

High Resolution Resistivity at 241-S Farm - Line 3E

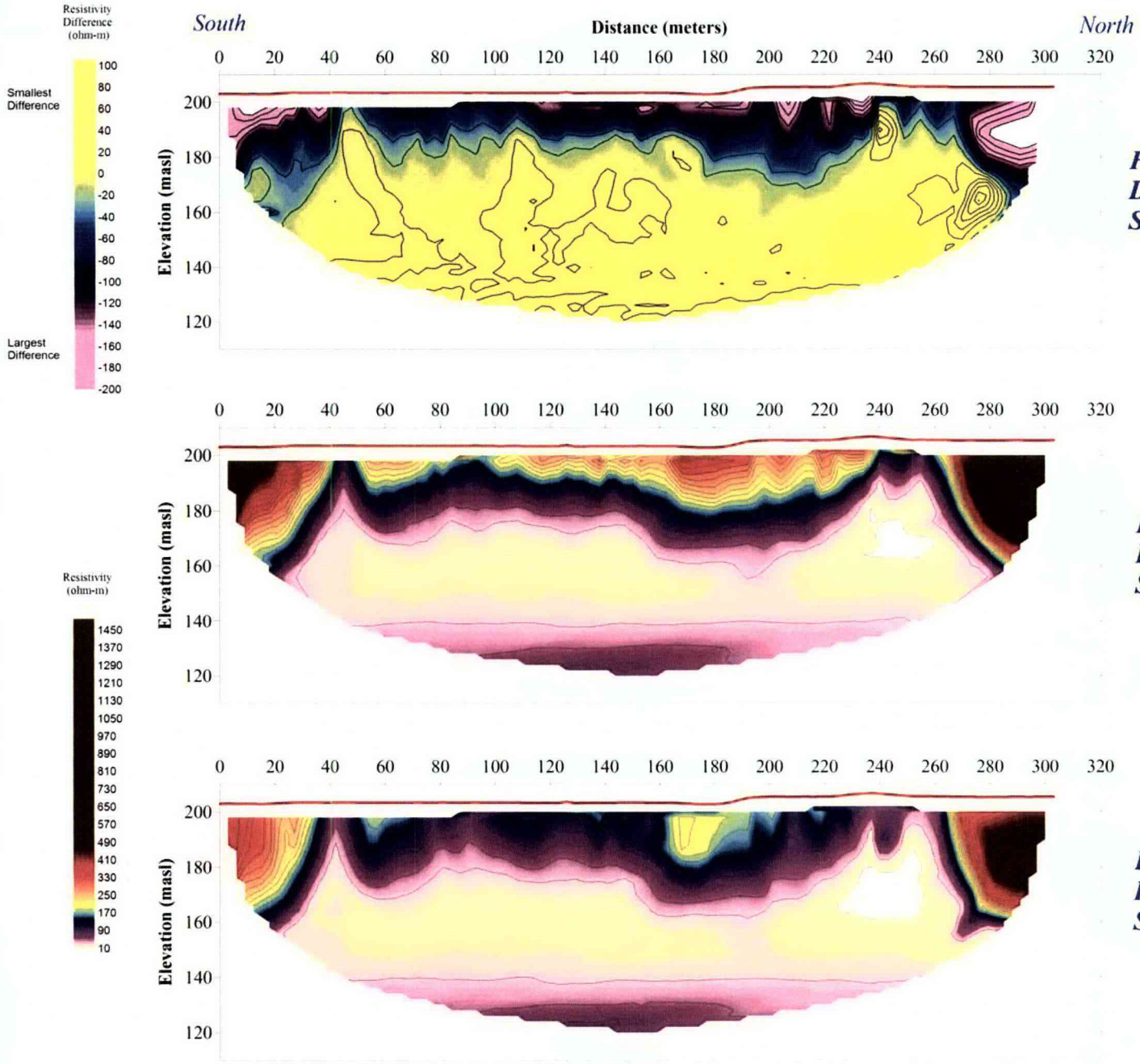

Map of Survey Lines

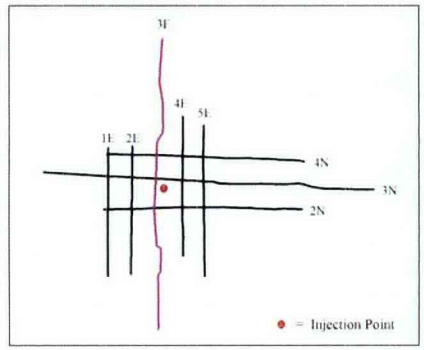

EQUIPMENT

Method: HRR
Rx/Tx: Advanced Geosciences Super Sting R8
Array: Pole-Pole
Spacing: 3 meter
Electrodes: 18" Stainless Steel

Scale: 1 in = 30 ft
Vertical Exaggeration: 1:1

0 15 30 45 60 75 90 105

Resistivity

CHG
241-S Farm
Hanford, WA

Date: Aug 2006 Figure: A -

High Resolution Resistivity at 241-S Farm - Line 3N

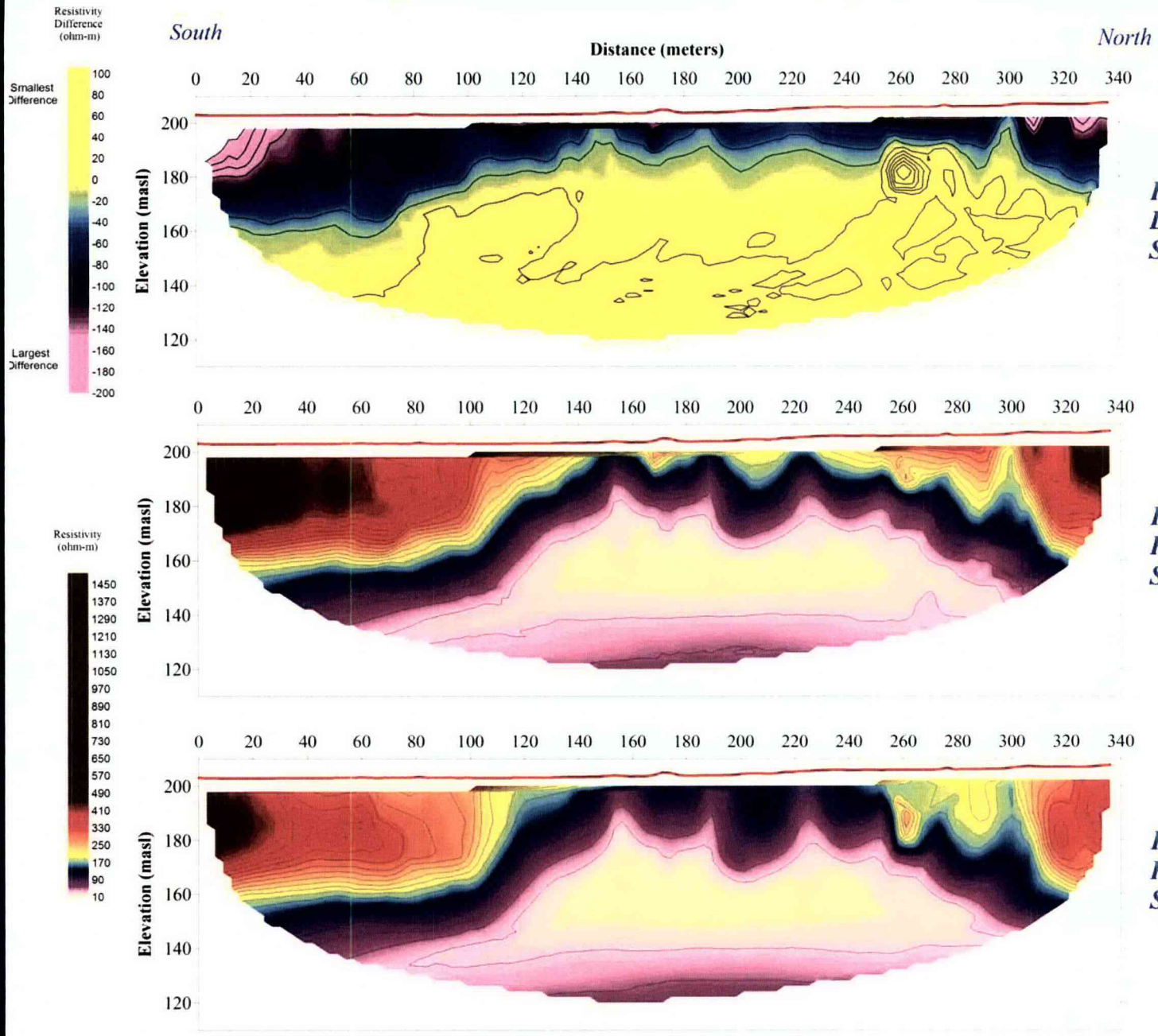

Map of Survey Lines

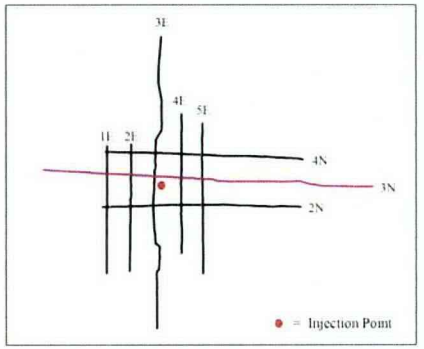

EQUIPMENT

Method: HRR
Rx/Tx: Advanced Geosciences Super Sting R8
Array: Pole-Pole
Spacing: 3 meter
Electrodes: 18" Stainless Steel

Scale: 1 in = 30 ft
Vertical Exaggeration: 1:1

0 15 30 45 60 75 90 105

Resistivity

CHG
241-S Farm
Hanford, WA

Date: *Aug 2006* Figure: A -

High Resolution Resistivity at 241-S Farm - Line 4E

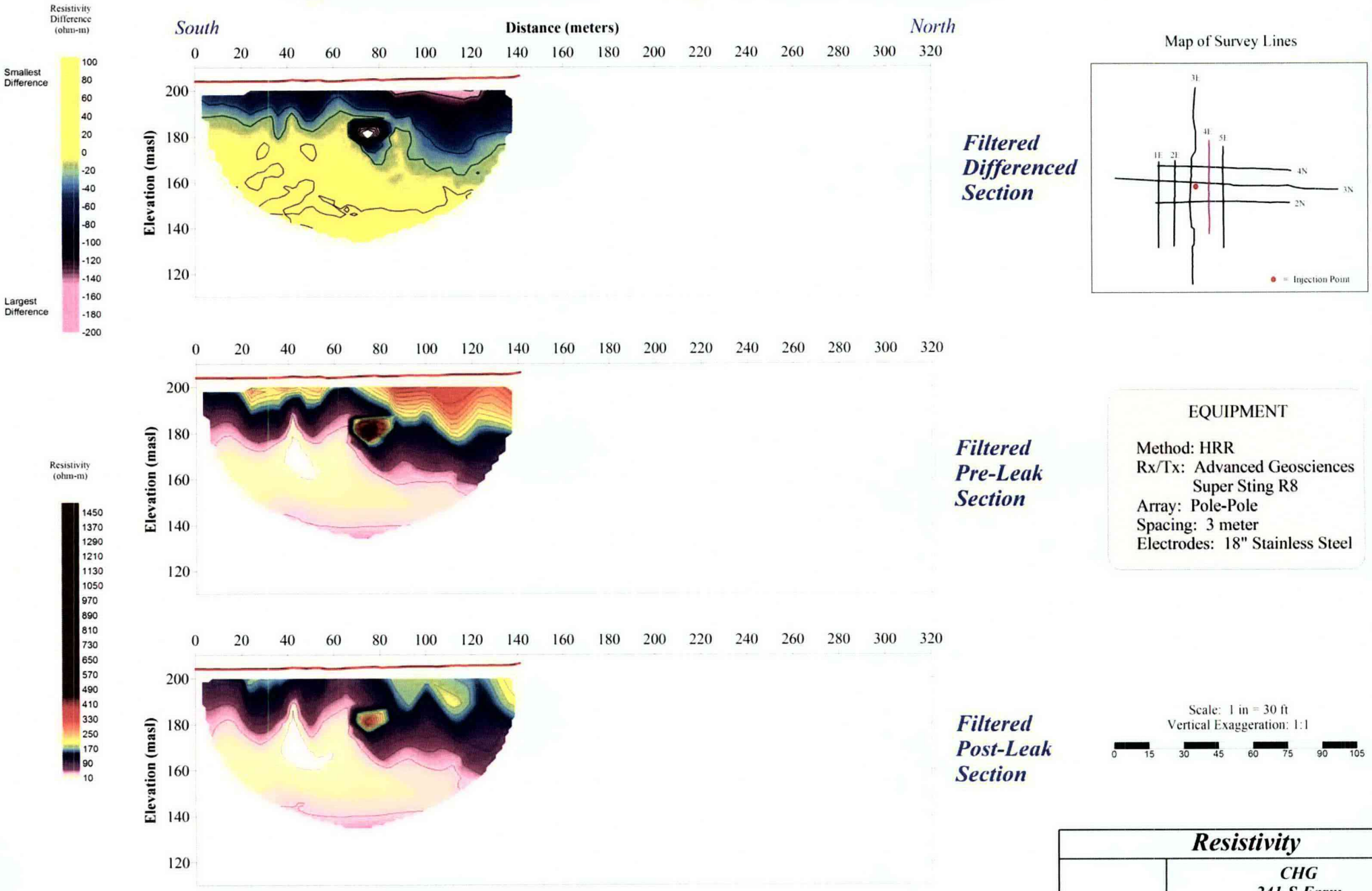

Resistivity

CHG
241-S Farm
Hanford, WA

Date: Aug 2006 Figure: A -

High Resolution Resistivity at 241-S Farm - Line 4N

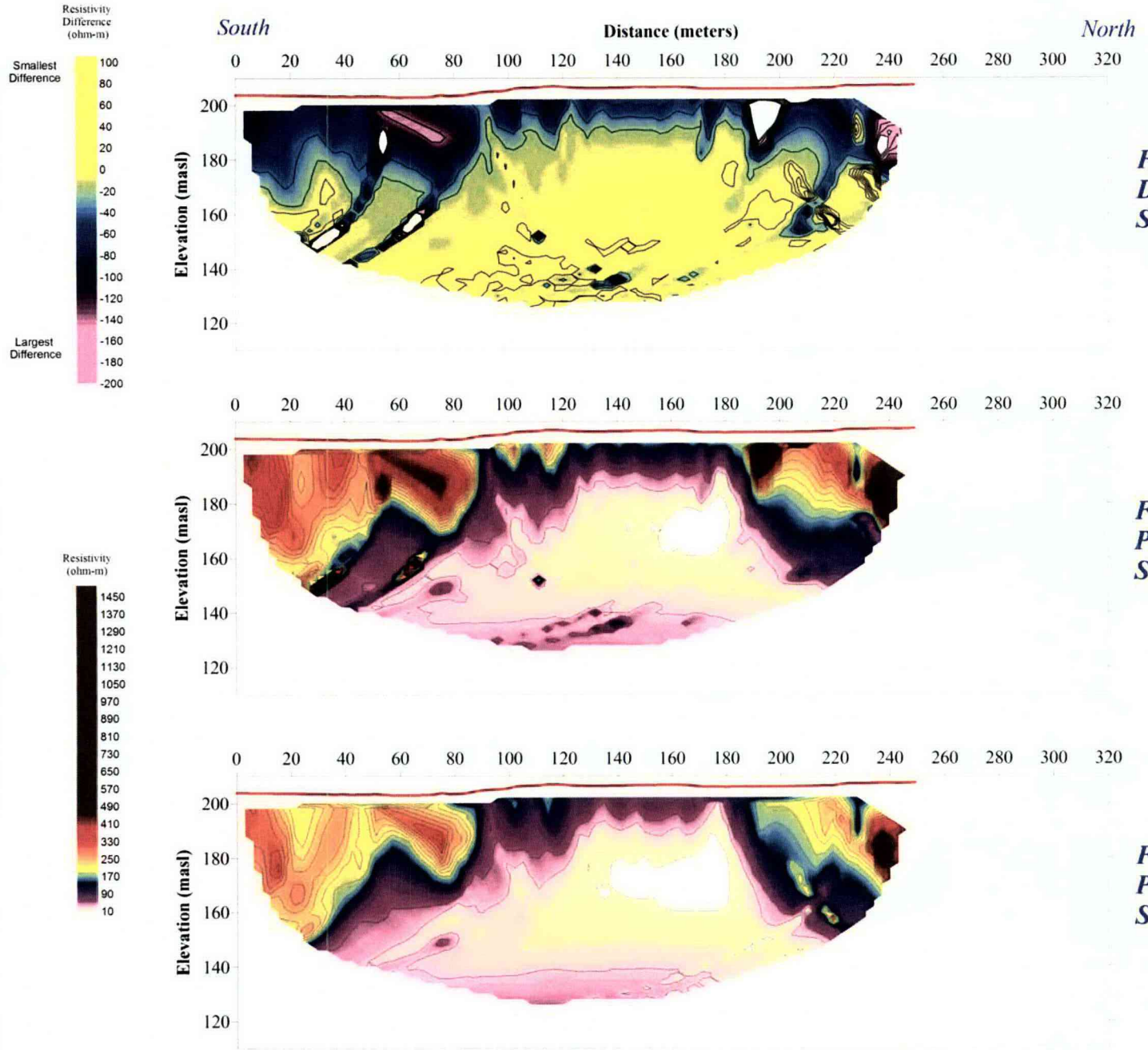

Map of Survey Lines

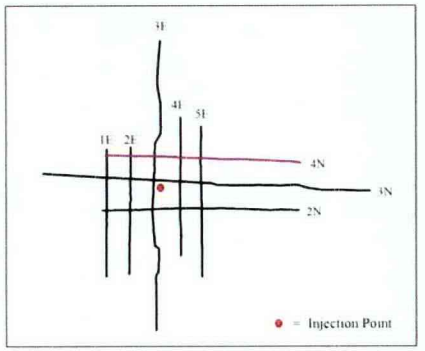

EQUIPMENT

Method: HRR
Rx/Tx: Advanced Geosciences Super Sting R8
Array: Pole-Pole
Spacing: 3 meter
Electrodes: 18" Stainless Steel

Scale: 1 in = 30 ft
Vertical Exaggeration: 1:1

0 15 30 45 60 75 90 105

Resistivity

CHG
241-S Farm
Hanford, WA

Date: Aug 2006 Figure: A -

High Resolution Resistivity at 241-S Farm - Line 5E

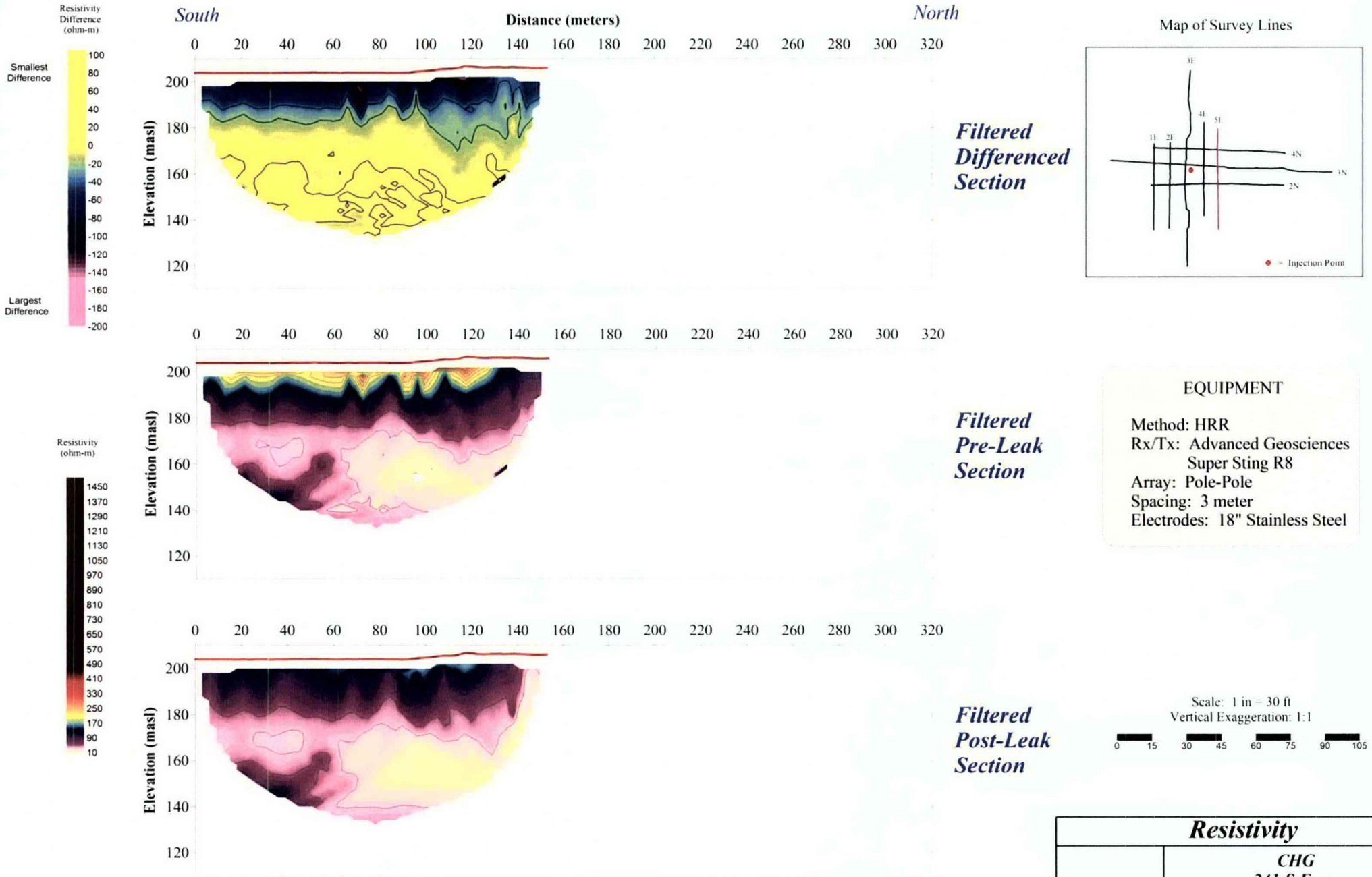

Map of Survey Lines

EQUIPMENT

Method: HRR
Rx/Tx: Advanced Geosciences Super Sting R8
Array: Pole-Pole
Spacing: 3 meter
Electrodes: 18" Stainless Steel

Scale: 1 in = 30 ft
Vertical Exaggeration: 1:1

0 15 30 45 60 75 90 105

Resistivity

CHG
241-S Farm
Hanford, WA

Date: Aug 2006 Figure: A -

Figure A-9. Electrical Resistivity Inversion at the 241-S Farm – Line 1E.

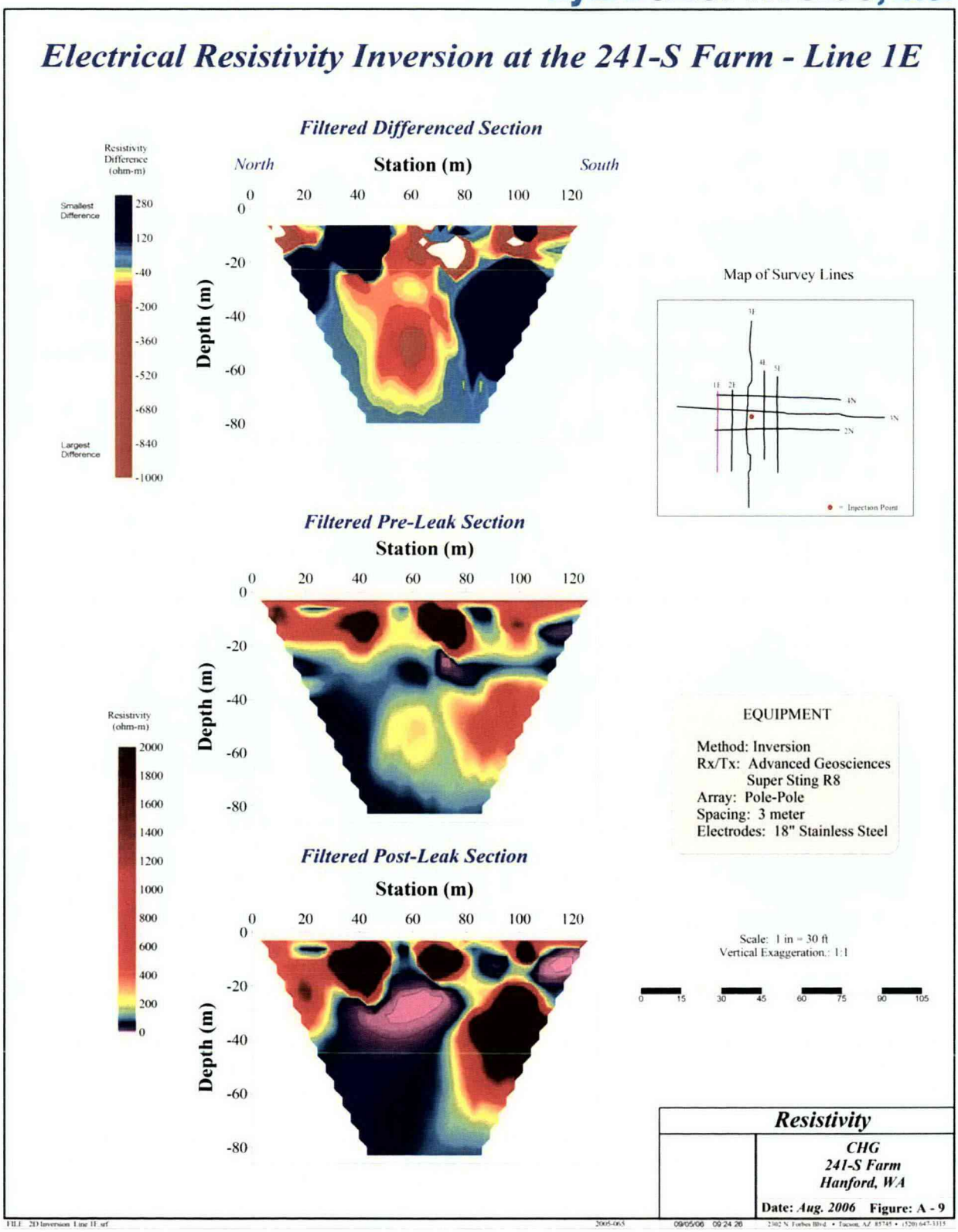

Figure A-10. Electrical Resistivity Inversion at the 241-S Farm – Line 2E.

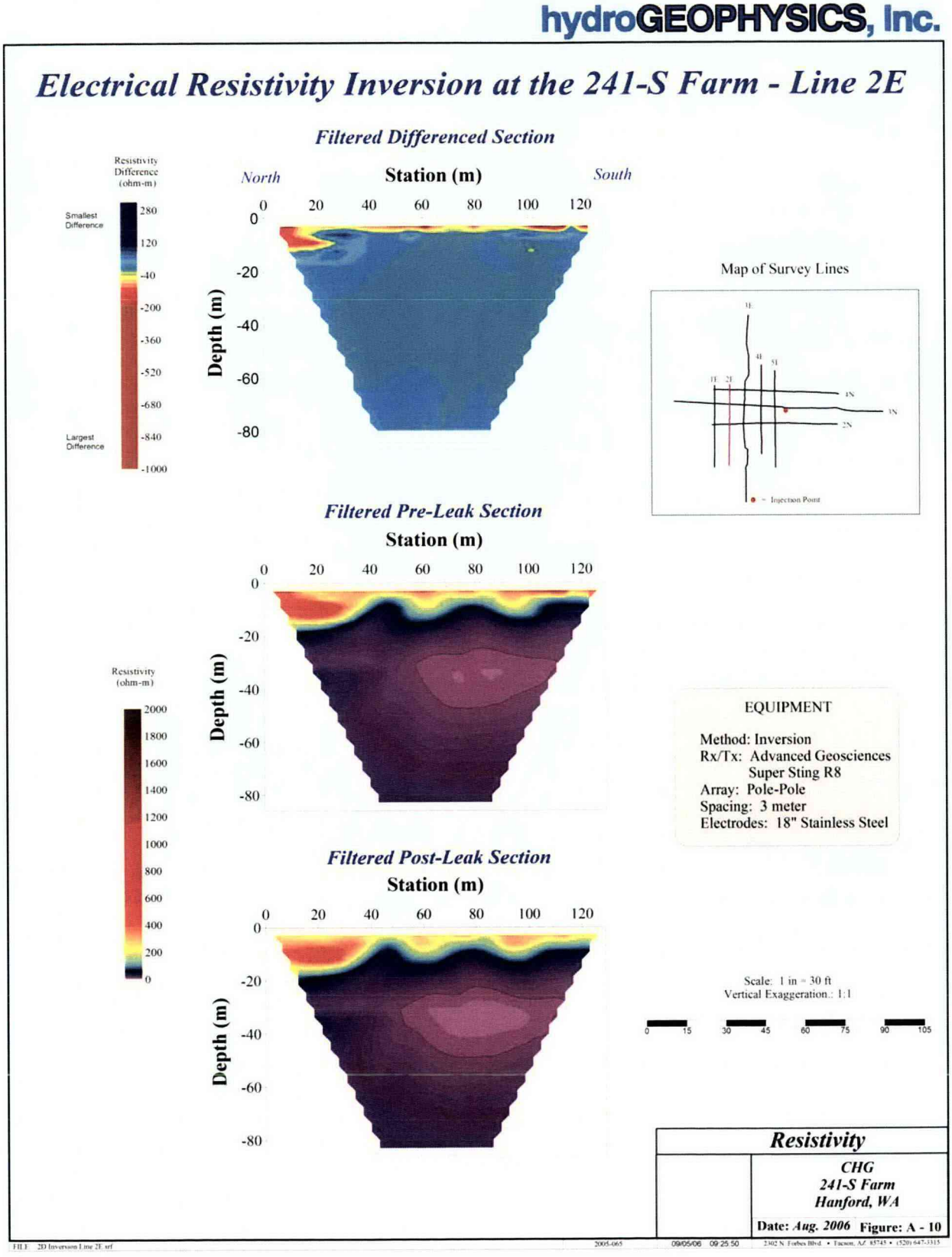

Figure A-11. Electrical Resistivity Inversion at the 241-S Farm – Line 2N.

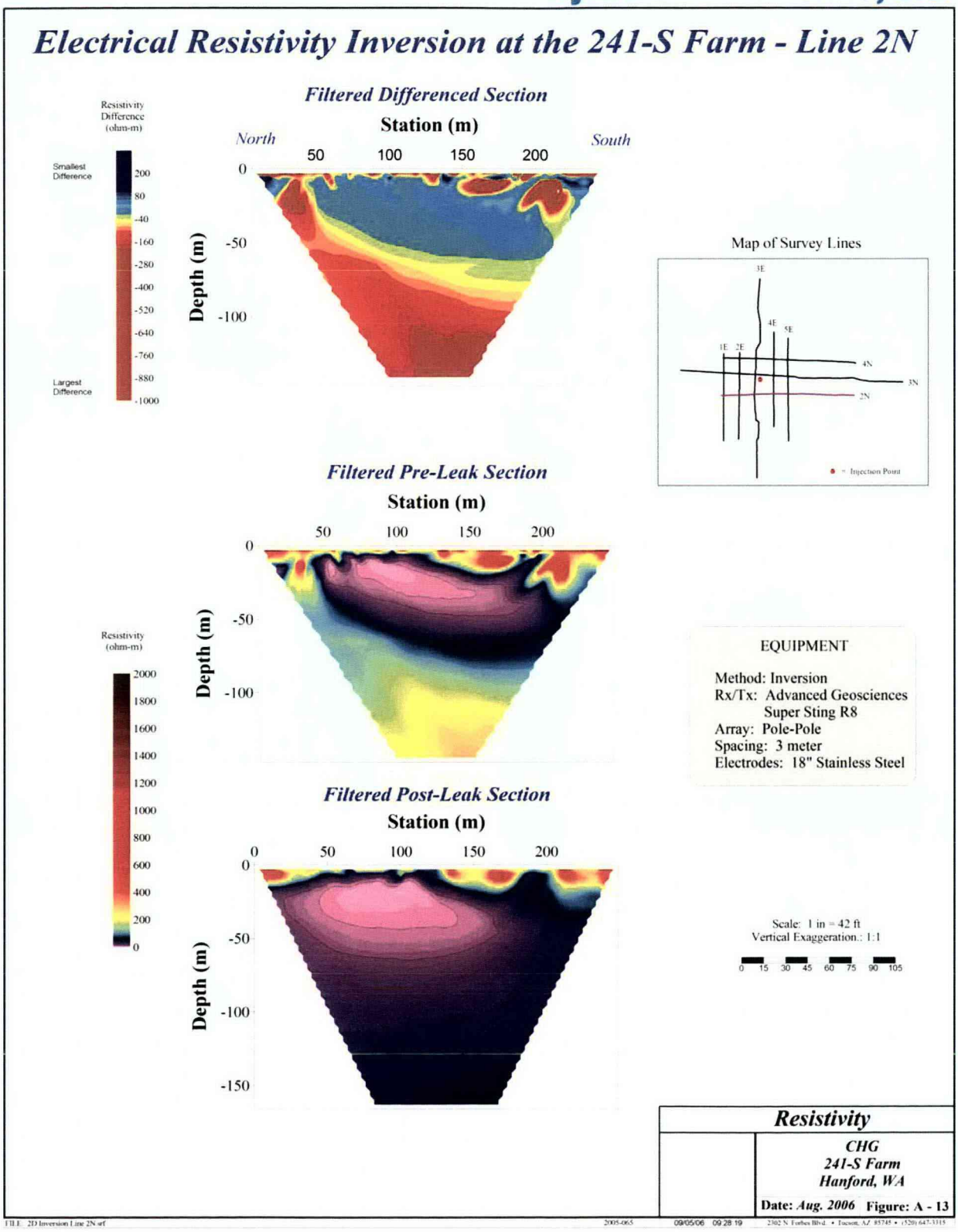

Figure A-12. Electrical Resistivity Inversion at the 241-S Farm – Line 3E.

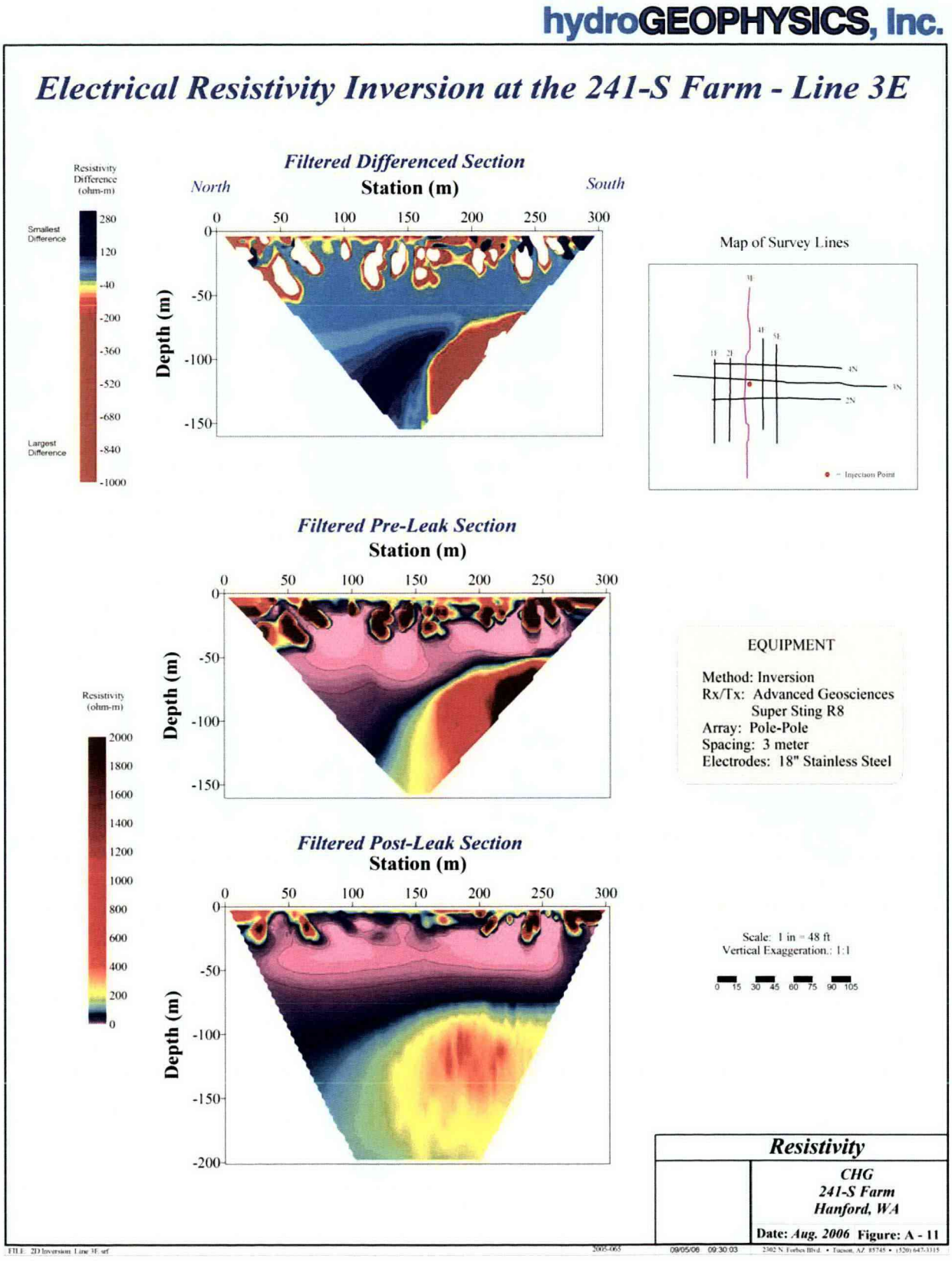

Figure A-13. Electrical Resistivity Inversion at the 241-S Farm – Line 3N.

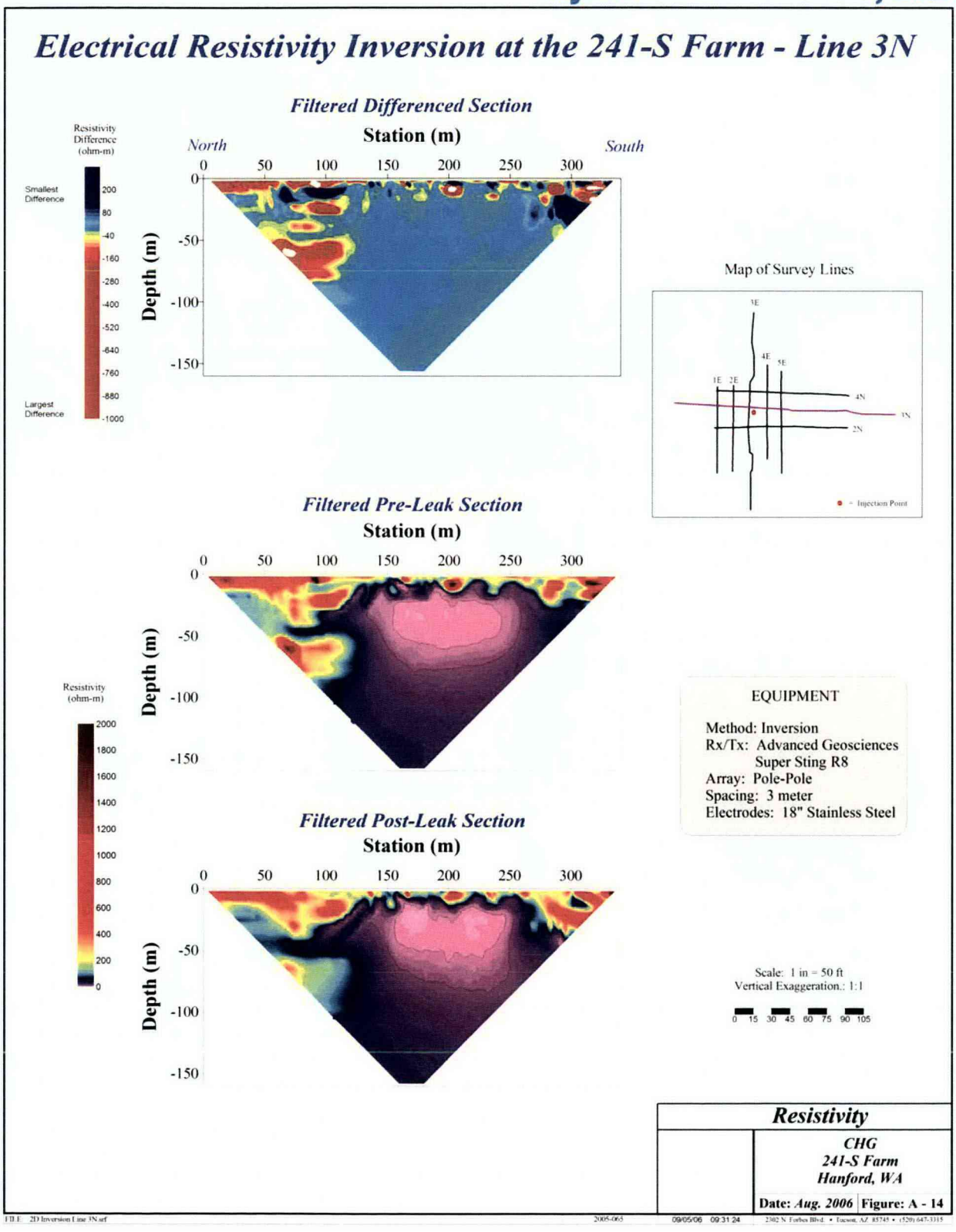

Figure A-14. Electrical Resistivity Inversion at the 241-S Farm – Line 4E.

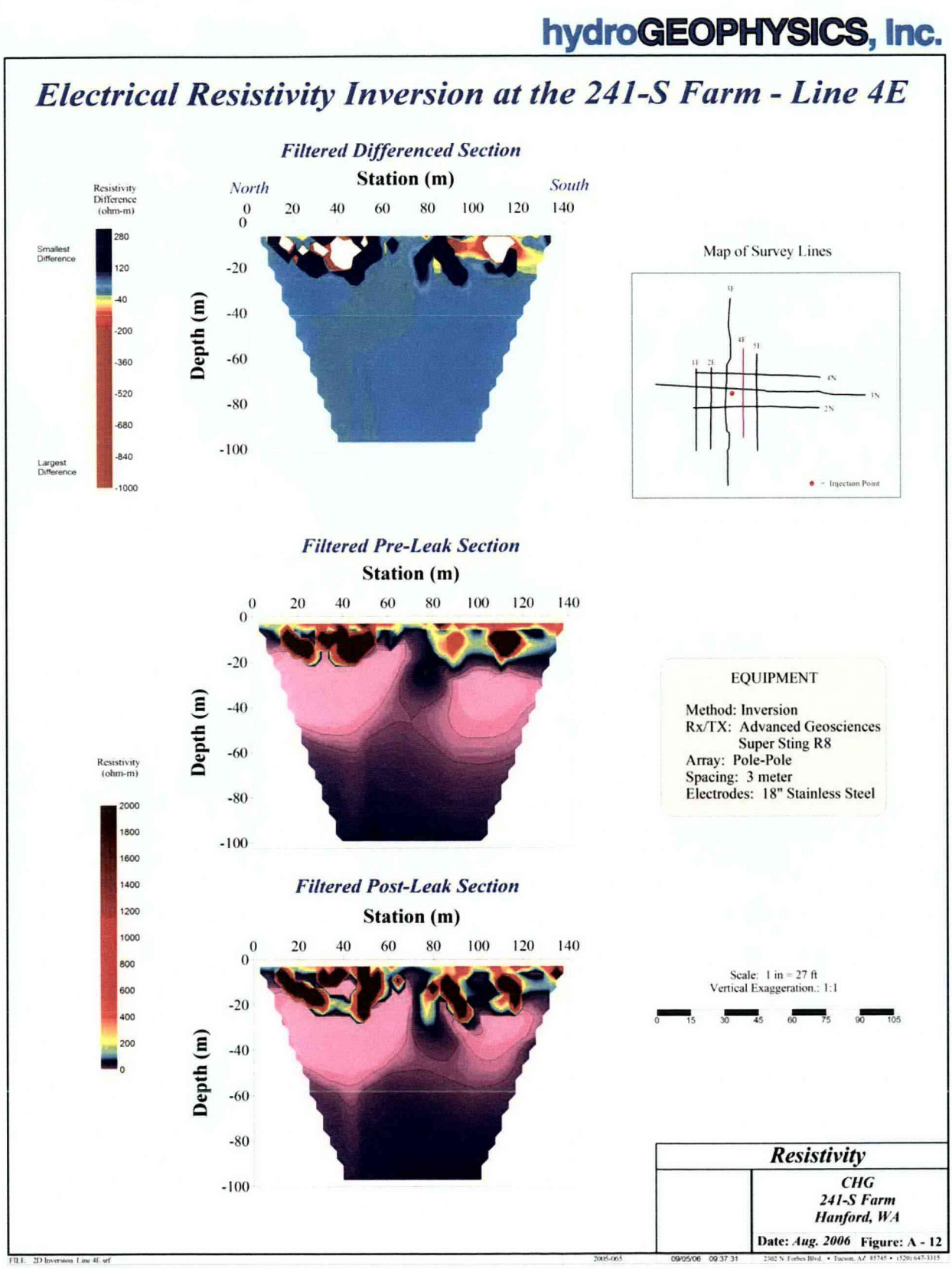

Figure A-15. Electrical Resistivity Inversion at the 241-S Farm – Line 4N.